University of Colorado, Boulder
CU Scholar

Spring 1-1-2014

Trajectory Optimization for Crewed Missions to an Earth-Moon L2 Halo Orbit

Jennifer Lynn Dowling

University of Colorado Boulder, jennifer.dowling@colorado.edu

Recommended Citation

Trajectory Optimization for Crewed Missions to an Earth-Moon L_2 Halo Orbit

by

Jennifer Dowling

B.S., Georgia Institute of Technology, 2012

A thesis submitted to the

Faculty of the Graduate School of the

University of Colorado in partial fulfillment

of the requirements for the degree of

Master of Science

Department of Aerospace Engineering Sciences

2014

This thesis entitled:
Trajectory Optimization for Crewed Missions to an Earth-Moon L_2 Halo Orbit
written by Jennifer Dowling
has been approved for the Department of Aerospace Engineering Sciences

_____

Jeffrey Parker

_____

Dr. George Born

_____

Dr. Jay McMahon

Date _____

The final copy of this thesis has been examined by the signatories, and we find that both the content and the form meet acceptable presentation standards of scholarly work in the above mentioned discipline.

Dowling, Jennifer (M.S., Aerospace Engineering Sciences)

Trajectory Optimization for Crewed Missions to an Earth-Moon L_2 Halo Orbit

Thesis directed by Dr. Jeffrey Parker

Baseline trajectories to an Earth-Moon L_2 halo orbit and round trip trajectories for crewed missions have been created in support of an advanced Orion mission concept. Various transfer durations and orbit insertion locations have been evaluated. The trajectories often include a deterministic mid-course maneuver that decreases the overall change in velocity in the trajectory. This paper presents the application of primer vector theory to study the existence, location, and magnitude of the mid-course maneuver in order to understand how to build an optimal round trip trajectory to an Earth-Moon L_2 halo orbit. The lessons learned about when to add mid-course maneuvers can be applied to other mission designs.

Dedication

To Scott, my family and friends for their encouragement and support.

Acknowledgements

Contents

Tables

Table

Figures

Figure

Chapter 1

Introduction

1.1   Motivation for Crewed Missions to L_2 Orbit

One concept for the next phase of human exploration of space includes a mission to the Earth-Moon Lagrange point L_2. This mission will be a test for the Orion vehicle in deep space and also allows different types of science to be performed while at the L_2 point. While at the L_2 point astronauts could remotely operate rovers on the far side of the moon, and could return samples from the Moon that were collected from the South Pole-Aitken basin.[1] These samples would be launched from the surface of the Moon and would rendezvous with the spacecraft at L_2.[12] Being in an orbit about the L_2 point will be the farthest that humans have gone from Earth, and will be a test that the Orion provides sufficient protection from deep space radiation. This mission is one of many missions that are seen as stepping stones to a goal of human exploration of Mars.[12]

1.2   Mission Design

The trajectories that were built to a halo orbit at L_2 took into account the necessary considerations for crewed flight. The length and ΔV requirements for this thesis are based on the Orion spacecraft, which is for four crew members, 21 days, and the total available spacecraft ΔV of 1340 m/s as seen in Table 1.1.[19]

These trajectories were built in segments, which can be seen in Figure 1.1 as different shades. The spacecraft exits its Earth orbit by performing a trans-lunar insertion burn and then performs a powered lunar flyby on its way to the halo orbit at L_2. To insert into the halo orbit, a halo

Table 1.1: Orion Spacecraft Capabilities

Total Duration	21 Days
Total ΔV	1340 m/s

orbit insertion (HOI) burn is performed. The spacecraft remains in the halo orbit for at least 5 days before exiting by performing a halo orbit exit (HOE) burn. The HOE starts the spacecraft on a return trajectory towards Earth. Another powered lunar flyby is performed and the spacecraft returns to Earth. The four burns that make up the total ΔV that the Orion spacecraft performs are: the outbound powered lunar flyby, halo orbit insertion burn, halo orbit exit burn and the inbound powered lunar flyby. The Interim Cryogenic Propulsion Stage will perform the trans-lunar insertion burn, rather than the Orion spacecraft.[19] As a result, this initial burn is not included in the total ΔV equation, as can be seen in Equation 1.1. The Earth to halo orbit trajectories only have two burns, the powered lunar flyby and halo orbit insertion burns, as shown in Equation 1.2.
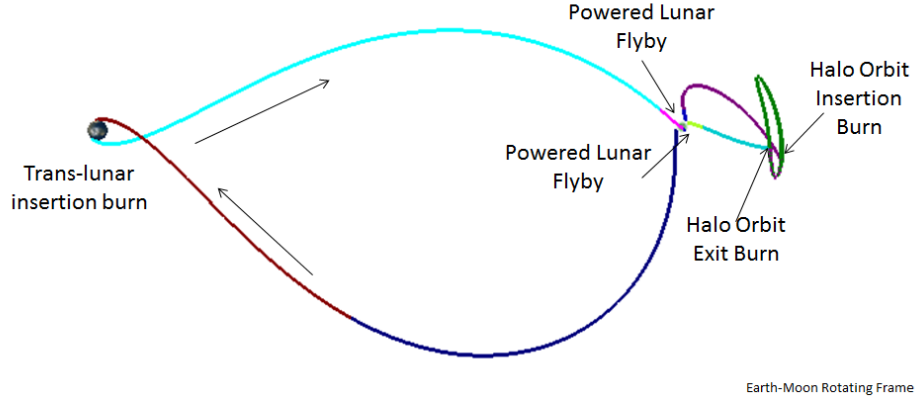
Figure 1.1: Round Trip Trajectory

$$\text{Total } \Delta V_{\text{Round Trip}} = \Delta V_{\text{Powered Lunar Flyby}} + \Delta V_{\text{Halo Orbit Insertion Burn}}$$
$$+ \Delta V_{\text{Halo Orbit Exit Burn}} + \Delta V_{\text{Powered Lunar Flyby}}$$

(1.1)

$$\text{Total } \Delta V_{\textbf{Earth to halo orbit}} = \Delta V_{\text{Powered Lunar Flyby}} + \Delta V_{\text{Halo Insertion Burn}} \qquad (1.2)$$

1.3   Background Information

1.3.1   Halo Orbits

A spacecraft can enter a periodic orbit about the Lagrange points in the Earth-Moon system, such as halo orbits.[19] Halo orbits are three dimensional orbits that when viewed from the Earth appear to make a halo around the Moon.[3] The halo orbit used in this thesis is defined in the Earth J2000 system at an epoch of August 24, 2021, and is a southern halo orbit. More information about the halo orbit is given in Chapter 3.

1.3.1.1 τ Angle Definition

The τ angle is defined by locating where the halo orbit crosses the y-axis, and is used in Chapter 4 to specify where the spacecraft enters the halo orbit. The first crossing is defined as the $0°$ angle and the second crossing is defined as $180°$. The halo orbit and the location of τ values of 0 and 180 degrees are shown in Figure 1.2. Using the amount of time between the y-axis crossings, a time per degree factor was calculated and used to find the day that other τ angles occurred. These day values are used as the time that the spacecraft enters the halo orbit.
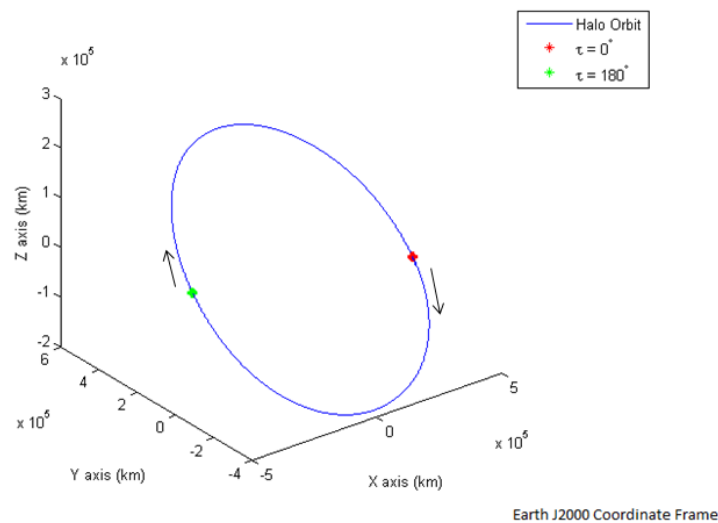
Figure 1.2: Halo Orbit with τ Angles Defined

1.3.2   Previous Trajectory Design for Crewed Mission to Earth-Moon L_2 Orbit

Pratt et al. designed 18 day and 31 day trajectories to a northern halo orbit at the Earth-Moon L_2 point. These trajectories had the spacecraft remain in the halo orbit for 5 days, and also included powered lunar flybys on the inbound and outbound legs. A mid-course maneuver was included between the Moon and halo orbit on both the outbound and inbound legs of the trajectory. The relationship between including a mid-course maneuver and the τ angle that the spacecraft enters was examined. When the halo orbit was entered at τ values between $90°$ and $270°$ the mid-course maneuver lowered the total ΔV. Knowing when to include the mid-course maneuver was uncertain and it was suggested that further investigation was needed to understand when a mid-course maneuver is needed.[19]

Trajectories that loop around L_2 or enter a Lissajous orbit were examined by Dunham et al. The trajectories that loop around L_2 spend approximately 10 days at L_2 and also include powered lunar flybys. The trajectories to the Lissajous orbit remain in the orbit for 5 revolutions about the L_2 point and then return to Earth. Lissajous orbit parameters that minimize Earth occultation times were also studied.[4]

1.4   Software Used

Two types of software were used in creating these trajectories and the subsequent analysis. The first was Copernicus[17], a spacecraft trajectory design and optimization software developed and used for many lunar mission designs and analyses by NASA/JSC. The second was a integrator function package called Turboprop[8].

1.4.1   Copernicus

Copernicus allows the user to create trajectories in segments. Each segment can be created using different initial conditions and can be propagated forwards or backwards in time. Examples of segments initial conditions are given in Tables 3.3 and 3.4. The time of each segment is defined

by three variables: initial time, duration and final time. Up to two of the three time variables can be used as optimization variables. In order to make a continuous trajectory, segment constraints can be added so that the segments match up. There are built-in optimizers available in Copernicus, including SNOPT[5], which is the optimizer used to help create the trajectories in this paper. A cost function can be defined, such as sum of maneuvers, and the optimizer will change the optimization variables in order to find a trajectory that not only minimizes the cost function but also satisfies the segment constraints. The cost function used in Copernicus to build these trajectories is the total ΔV defined in Equation 1.1 or 1.2. Copernicus comes with Matlab functions that allow the initial conditions and other variables of each segment to be read in and used in Matlab.

1.4.2   TurboProp

TurboProp was created at Colorado Center for Astrodynamics Research (CCAR), and is a package of functions with integrators that use a variety of models, including the JPL planetary ephemerides[9]. There is an option to calculate the state transition matrix which is needed to calculate the primer vector of the trajectory. TurboProp was used as a tool to recreate the trajectories built in Copernicus and to calculate the primer vector for the trajectory, for plotting and analysis. Turboprop is used with the optimizer fmincon[16] in the round trip trajectories. The optimizer is used to rebuild the trajectories built in Copernicus and to add in mid-course maneuvers in different ways. These round trip trajectories are discussed in Chapter 4.

1.5   Thesis Organization

This thesis will address when additional maneuvers are beneficial to a trajectory that inserts a spacecraft into a halo orbit about the L_2 point and returns to Earth. First the Earth to halo portion of the trajectory is focused on in Chapter 3, then round trip trajectories, going from the Earth to the halo orbit and returning to Earth, are focused on in Chapter 4. At times adding a mid-course maneuver in the trajectories between the Moon and halo orbit is beneficial in reducing the total ΔV, but this is not true for every case. In the Earth to halo orbit trajectories, the focus

was on determining when these mid-course maneuvers (MCM), after the powered lunar flyby and before halo orbit insertion, are beneficial, when they are not, and where they are best placed in the trajectory. The round trip trajectories were examined to see if there are other beneficial locations of adding a mid-course maneuver in the trajectory, including in the Moon to halo orbit or halo orbit to Moon portion. These trajectories were built in the Earth J2000 system at a reference epoch of August 16, 2021.[19] The force model used to create these trajectories includes point-mass gravitational forces from the Earth, Moon and Sun. The planets positions were calculated by Copernicus[17] and Turboprop[8] using the JPL Planetary and Lunar Ephemerides DE405[9].

In order to create an optimal trajectory to a L_2 halo orbit, primer vector theory will be used, which is described in Chapter 2. Primer vector theory (PVT) is a trajectory optimization tool developed by Lawden[14, 13] and expanded upon by many. Lion and Handelsman[15] developed conditions where an additional impulse can improve a trajectory, and Davis[3] adapted primer vector theory for the circular restricted three body problem. The criteria for an additional impulse will be used to illustrate when a mid-course maneuver is beneficial to a trajectory and when it is not needed. Primer vector theory gives a first order estimate of the best location of the additional impulse, which in this case is a mid-course maneuver. The location and magnitude of an additional impulse can be calculated by primer vector theory and this method is used in the round trip trajectories in addition to the first order estimate of the best location.[3]

Chapter 2

Primer Vector Theory

Primer vector theory is introduced and derived in this chapter. Calculations for location and magnitude of an additional impulse are derived for application in the round trip trajectories. Previous applications of primer vector theory are outlined and examined.

2.1 Derivation of Primer Vector Theory

The primer vector is defined as the adjoint to the velocity vector.[3] Primer vector theory can be applied to trajectories that have an impulsive initial and final ΔV. The optimal criterion for primer vector theory and cost function is shown in Equation (2.1).[3]

$$J = \sum_{i=1}^{N} |\Delta \overline{V_i}| \tag{2.1}$$

The derivation of primer vector theory in an inertial two body frame was done by Jezewski [10]. The following derivation and explanations in Equations 2.4 to 2.28 is an abbreviated version of his derivation with some notation changes. The state equations for the trajectory problem are:

$$\dot{\overline{V}} = \frac{\beta c \overline{\ell}}{m} + \overline{G} \tag{2.2}$$

$$\dot{\overline{R}} = \overline{V} \tag{2.3}$$

$$\dot{m} = -\beta \tag{2.4}$$

$\overline{R}$ is the position vector, $\overline{V}$ is the velocity vector and $\overline{G}$ is the gravity vector. βc is thrust magnitude, β is the mass flow rate, c is the exhaust velocity and m is the spacecraft mass. The direction cosine vector $\overline{\ell}$ is constrained by the relationship in Equation 2.5.

$$\overline{\ell}^T \overline{\ell} = 1 \tag{2.5}$$

The mass flow rate is constrained by the relationship in Equation 2.6 in which α is defined as a slack variable.

$$\beta(\beta_{max} - \beta) = \alpha^2 \geq 0 \tag{2.6}$$

The Hamiltonian function is defined in Equation 2.7 where $\overline{P}$ and $\overline{Q}$ are vectors and η, μ_1 and μ_2 are scalars and time varying Lagrange multipliers. $\overline{P}$ is the primer vector.

$$H = \overline{P}^T \left(\frac{\beta c \overline{\ell}}{m} + \overline{G} \right) + \overline{Q}^T V - \eta\beta - \mu_1 \left(\overline{\ell}^T \overline{\ell} - 1 \right) - \mu_2 \left(\beta \left(\beta_{max} - \beta \right) - \alpha^2 \right) \tag{2.7}$$

The necessary conditions for an optimal trajectory are as follows:

$$\dot{\overline{P}} = -\frac{\partial H}{\partial \overline{V}} = -\overline{Q}^T \tag{2.8}$$

$$\dot{\overline{Q}}^T = -\frac{\partial H}{\partial \overline{R}} = -\overline{P}^T \frac{\partial \overline{G}}{\partial \overline{R}} \tag{2.9}$$

$$\dot{\eta} = -\frac{\partial H}{\partial m} = \frac{\beta c}{m^2} \overline{P}^T \overline{\ell} \tag{2.10}$$

$$0 = -\frac{\partial H}{\partial \overline{\ell}} = -\frac{\beta c}{m} \overline{P}^T + 2\mu_1 \overline{\ell}^T \tag{2.11}$$

$$0 = -\frac{\partial H}{\partial \beta} = -\frac{c}{m} \overline{P}^T \overline{\ell} + \eta + \mu_2(\beta_{max} - 2\beta) \tag{2.12}$$

$$0 = -\frac{\partial H}{\partial \alpha} = -2\mu_2 \alpha \tag{2.13}$$

From Equation 2.13, $\mu_2 = 0$ or $\alpha = 0$ or $\mu_2 = \alpha = 0$. If:

$$\alpha = 0 \Rightarrow \left\{ \begin{array}{c} \beta = 0 \\ \text{or} \\ \beta = \beta_{max} \end{array} \right\} \tag{2.14}$$

If $\alpha \neq 0$ and $\mu_2 = 0$ then $0 < \beta < \beta_{max}$. Thus the solution may have the following three types of arcs:

(1) Maximum Thrust (MT)

(2) Null Thrust (NT)

(3) Intermediate Thrust (IT), singular arc

From Equation 2.11, the following conditions become apparent.

(1) If $\beta \neq 0$ and $\mu_1 \neq 0$, $\overline{P}$ and $\bar{\ell}$ are parallel.

(2) If $\beta = 0$ and $\mu_1 = 0$, $\bar{\ell}$ is indeterminate.

(3) If $\mu_1 = 0$ and $\beta \neq 0$, $\overline{P}$ vanishes.

Investigating if $\overline{P}$ and $\bar{\ell}$ are parallel in the same or opposing directions is investigated using the Weierstrass condition, but is omitted here, for further details see Reference [10]. For the maximum thrust arc $\overline{P}$ is aligned with $\bar{\ell}$. From this derivation the necessary conditions for an optimal impulsive trajectory are found. These conditions are listed below as stated by Jezewski and Rozendaal:[11]

(1) The primer vector and its first derivative are everywhere continuous.

(2) Whenever an impulse occurs, the primer vector is aligned with the impulse and has unit magnitude.

(3) The primer vector magnitude must never exceed unity on a coasting arc.

(4) The time derivative of the primer vector magnitude must be zero at all interior junction points separating coasting arcs.

A primer magnitude that has a maximum value greater than 1 indicates that an additional impulse is beneficial. In order to investigate this further, Jezewski develops an adjoint equation by doing the following:

$$\dot{\overline{R}} = \overline{V} \tag{2.15}$$

$$\dot{\overline{V}} = \overline{\nabla} U(\overline{R}, t) \tag{2.16}$$

U is the potential and $\overline{\nabla}$ is the gradient operator. A variation between a perturbed and reference trajectory is represented as δ, for example, $\delta\overline{R} = \overline{R}' - \overline{R}$. $\overline{R}'$ is the position of the perturbed trajectory and $\overline{R}$ is the position of the reference or original trajectory. Taking variations in Equations 2.15 and 2.16 this results with:

$$\left.\begin{matrix} \begin{bmatrix} \delta\dot{\overline{R}} \\ \delta\dot{\overline{V}} \end{bmatrix} = A \begin{bmatrix} \delta\overline{R} \\ \delta\overline{V} \end{bmatrix} \\ A = \begin{bmatrix} 0 & I \\ G & 0 \end{bmatrix} \end{matrix}\right\} \tag{2.17}$$

In Equation 2.17 I is the identity matrix and G is the gravity gradient matrix. G is of the form in Equation 2.18 where i and $j = 1, 2, 3$.

$$\overline{g}_{ij} = \frac{\partial^2 U(\overline{R}, t)}{\partial \overline{R}_i \partial \overline{R}_j} \tag{2.18}$$

The system of equations adjoint to Equation 2.17 is:

$$\begin{bmatrix} \dot{\overline{\varphi}} \\ \dot{\overline{\lambda}} \end{bmatrix} = -A^T \begin{bmatrix} \overline{\varphi} \\ \overline{\lambda} \end{bmatrix} \tag{2.19}$$

φ and λ are adjoint variables. λ is the adjoint to the velocity vector and is therefore the primer vector and will be written here as $\overline{P}$. Writing equations 2.17 and 2.19 in second order form results in:

$$\left.\begin{aligned} \delta\ddot{\overline{R}} &= G\delta\overline{R} \\ \ddot{\overline{P}} &= G\overline{P} \end{aligned}\right\} \tag{2.20}$$

Next premultiply the first equation by $\overline{P}^T$ and second equation by $\delta\overline{R}^T$ and then subtract the equations in Equation 2.20. This results in,

$$\overline{P}^T\delta\ddot{\overline{R}} - \delta\overline{R}^T\ddot{\overline{P}} = \overline{P}^T G\delta\overline{R} - \delta\overline{R}^T G\overline{P} = 0 \tag{2.21}$$

Further simplification allows the equation to be expressed as a time derivative as seen in Equation 2.22.

$$\frac{d}{dt}(\overline{P}^T\delta\overline{V} - \dot{\overline{P}}^T\delta\overline{R}) = 0 \tag{2.22}$$

Integrating the above equation, you obtain the adjoint equation shown in Equation 2.23.

$$\overline{P}^T\delta\overline{V} - \dot{\overline{P}}^T\delta\overline{R} = \text{constant} \tag{2.23}$$

This relationship applies for the interval between any two impulses and is used to derive the calculations for the location of an additional impulse.

The state variable perturbations at any two times between impulses are related by the state transition matrix:

$$\begin{bmatrix} \delta\overline{R}(t) \\ \delta\overline{V}(t) \end{bmatrix} = \Phi(t, t_0) \begin{bmatrix} \delta\overline{R}(t_0) \\ \delta\overline{V}(t_0) \end{bmatrix} \tag{2.24}$$

$$\begin{bmatrix} \delta\overline{R}(t) \\ \delta\overline{V}(t) \end{bmatrix} = \begin{bmatrix} \Phi_{1,1}(t, t_0)_{3\times3} & \Phi_{1,2}(t, t_0)_{3\times3} \\ \Phi_{2,1}(t, t_0)_{3\times3} & \Phi_{2,2}(t, t_0)_{3\times3} \end{bmatrix} \begin{bmatrix} \delta\overline{R}(t_0) \\ \delta\overline{V}(t_0) \end{bmatrix} \tag{2.25}$$

The state transition matrix is numerically integrated for these trajectories. The primer vector can also be transformed in the same manner as the state variables as can be seen in Equation 2.26.

$$\begin{bmatrix} \overline{P}(t) \\ \dot{\overline{P}}(t) \end{bmatrix} = \begin{bmatrix} \Phi_{1,1}(t,t_0)_{3\times3} & \Phi_{1,2}(t,t_0)_{3\times3} \\ \Phi_{2,1}(t,t_0)_{3\times3} & \Phi_{2,2}(t,t_0)_{3\times3} \end{bmatrix} \begin{bmatrix} \overline{P}(t_0) \\ \dot{\overline{P}}(t_0) \end{bmatrix} \tag{2.26}$$

At the time of each impulse the primer vector is defined by Equation 2.27, and the primer magnitude is unity.

$$\left.\begin{aligned} \overline{P}(t_0) = \frac{\Delta\overline{V}_0}{|\,\Delta\overline{V}_0\,|} \\ \overline{P}(t_f) = \frac{\Delta\overline{V}_f}{|\,\Delta\overline{V}_f\,|} \end{aligned}\right\} \tag{2.27}$$

Using Equation 2.27 as boundary conditions, the derivative of primer vector at the initial time can be found using Equation 2.28.

$$\dot{\overline{P}}(t_0) = \Phi_{1,2}^{-1}(t_f,t_0)[\overline{P}(t_f) - \Phi_{1,1}(t_f,t_0)\overline{P}(t_0)] \tag{2.28}$$

Using Equation 2.27 and 2.28 the primer vector can be mapped throughout the trajectory. Then the primer magnitude is plotted to see if the magnitude exceeds one.

2.2 Calculations for Location and Magnitude of an Additional Impulse

When the primer magnitude exceeds one, this indicates that an additional impulse would be beneficial to the trajectory. Lion and Handelsman [15] extended the use of primer vector theory to show that when the primer magnitude exceeds 1, an additional impulse may be used to reduce the total ΔV. The original two impulse trajectory has a higher cost than the resulting three impulse trajectory. To get the maximum improvement in cost to the first order, the impulse should be placed at the time the maximum primer magnitude occurs.[15]

Primer vector theory can be used to calculate the location and magnitude of the additional impulse. The original trajectory, referred to as the reference trajectory, has an area where the primer magnitude peaks and exceeds one. This trajectory will be perturbed, and its cost will be denoted as J'. The perturbed trajectory will go through the location of the additional impulse $\overline{R}_m + \delta\overline{R}_m$, where $\overline{R}_m$ is the location of maximum primer magnitude in the reference trajectory

at time t_m. The perturbed and reference trajectory have the same initial and final positions, the difference between the trajectories at the initial and final time is the ΔV's that are applied at those locations.[3] To find the change in cost (J) between the reference trajectory and perturbed trajectory, the following equations are defined. $\overline{P}_m$ is the maximum primer vector. The following Equations 2.29 to 2.32 are a shortened derivation from Jezeweski.[10]

$$\left.\begin{aligned} C &=\mid \Delta\overline{V}_m \mid \\ \Delta &= \frac{\Delta\overline{V}_m}{C} \end{aligned}\right\} \tag{2.29}$$

$$\delta J = C(1 - \overline{P}_m^T \Delta) \tag{2.30}$$

When $|\overline{P}_m|$ is greater than 1 then the change in cost is less than zero, which indicates that the cost of the two impulse trajectory is greater than the cost of the three impulse trajectory. Therefore to the first order the greatest cost savings can be found by applying the maneuver when $P = P_{max}$. After the impulse is added the primer magnitude of the three impulse trajectory should be examined to see if the primer magnitude is greater than 1 at any time, and therefore the location of the impulse should be changed.

To find out how much the reference trajectory should be perturbed, and in what direction further derivation is done. This results in Equation 2.32, which illustrates how much the location of maximum primer magnitude should be altered.

$$A = \Phi_{2,2}(t_m, t_f)\Phi_{1,2}^{-1}(t_m, t_f) - \Phi_{2,2}(t_m, t_0)\Phi_{1,2}^{-1}(t_m, t_0) \tag{2.31}$$

$$\delta\overline{R}_m = CA^{-1}\frac{\overline{P}_m}{|\overline{P}_m|} \tag{2.32}$$

Jezewski uses a second order cost function variation to find C, which is a function of the state transition matrix. However, since the state transition matrix can be computed numerically, an abbreviated different solution is found in Equations 2.33 to 2.40 following a derivation and explanation by Davis [3]. First, the cost function of the perturbed trajectory is examined in Equation 2.33.

$$J' =\mid \Delta\overline{V}_0 + \delta\overline{V}_0 \mid + \mid \Delta\overline{V}'_m \mid + \mid \Delta\overline{V}_f - \delta\overline{V}_f \mid \tag{2.33}$$

$$\delta\overline{V}_0 = C\Phi_{1,2}^{-1}(t_m, t_0)A^{-1}\frac{\overline{P}_m}{\mid \overline{P}_m \mid} \tag{2.34}$$

$$\delta\overline{V}_f = C\Phi_{1,2}^{-1}(t_m, t_f)A^{-1}\frac{\overline{P}_m}{\mid \overline{P}_m \mid} \tag{2.35}$$

To simplify further, the vectors $\overline{\alpha}$ and $\overline{\beta}$ are defined as the following:

$$\overline{\alpha} = \Phi_{1,2}^{-1}(t_m, t_0)A^{-1}\frac{\overline{P}_m}{\mid \overline{P}_m \mid} \tag{2.36}$$

$$\overline{\beta} = C\Phi_{1,2}^{-1}(t_m, t_f)A^{-1}\frac{\overline{P}_m}{\mid \overline{P}_m \mid} \tag{2.37}$$

The above equations can be inserted into 2.34 and 2.35 to simplify to:

$$\delta\overline{V}_0 = C\overline{\alpha} \tag{2.38}$$

$$\delta\overline{V}_f = C\overline{\beta} \tag{2.39}$$

Substituting Equations 2.38 and 2.39 into the perturbed cost function in Equation 2.33 yields the following:

$$\left.\begin{array}{r}J' =\mid \Delta\overline{V}_0 + C\overline{\alpha} \mid +C+ \mid \Delta\overline{V}_f - C\overline{\beta} \mid \\ J' = (\Delta\overline{V}_0^T\Delta\overline{V}_0 + 2C\overline{\alpha}^T\Delta\overline{V}_0 + C^2\overline{\alpha}^T\overline{\alpha})^{1/2} + (\Delta\overline{V}_f^T\Delta\overline{V}_f - 2c\beta^T\Delta\overline{V}_f + C^2\overline{\beta}^T\overline{\beta})^{1/2} + C\end{array}\right\} \tag{2.40}$$

The magnitude of the impulsive maneuver can be solved for iteratively to find the C value that minimizes J' using Equation 2.40.

While this technique can be used to get the location of the impulse, the resulting three impulse trajectory might not be optimal. The primer plot of the resulting trajectory will need to be investigated to see if any further changes are required.[3]

2.2.1   Using Primer Vector Theory with Multiple Point Masses

Guzmán [6] investigated using primer vector theory in various force models and frames. This was done to understand which force models and frames can be used with primer vector theory, and if any changes to the derivation of the primer vector are required for it to be used. He found that adding other point mass perturbations satisfies the required equations and no changes are needed before implementation.

Two equations were used to check if primer vector theory in different frames and force models could be used. These equations were derived in the rotating frame, therefore there are two G variables, G_r which was previously called G, and G_v which is not found in inertial frames. The first equation, shown in Equation 2.41 uses both of the G terms, and is followed by Equation 2.17 except that the bottom right value in the matrix is not zero, but is G_v. If this equation is not satisfied, than the state transition matrix cannot be used to map the primer vector across the trajectory. The following equations and explanations follow the derivation done by Guzmán in the rotating frame:[6]

$$(G_r - \dot{G}_v)^T = G_r$$
$$G_v^T = -G_v$$

$$(2.41)$$

The second equation that has to be satisfied is Equation 2.44 which checks that the time and position are continuous over an impulse. The following equations illustrate how this is checked:

$$\overline{g}(t, \overline{r}, \overline{v}) = \overline{g}_1(t, \overline{r}) + \overline{g}_2(t, \overline{v}) \tag{2.42}$$

where $\overline{g}_1$ and $\overline{g}_2$ are force model dependent. g_2 can be expressed as:

$$\overline{g}_2(t, \overline{v}) = G_v(t)\overline{v}$$
$$G_v = \frac{\partial \overline{g}}{\partial \overline{v}} = \frac{\partial \overline{g}_2}{\partial \overline{v}}$$

$$(2.43)$$

Equation 2.42 can be rewritten as:

$$\overline{g}(t, \overline{r}, \overline{v}) = \overline{g}_1(t, \overline{r}) - G_v(t)\overline{v} \tag{2.44}$$

Since $\bar{g}_1$ is only a function of time and position, it is continuous across an impulse.

When there are multiple bodies used, there are N point masses, the spacecraft is the i-th and it does not affect the motion of the other point masses, and the central body is the q-th. The perturbing gravity potential is given by the following equation,

$$U_{\text{point masses}} = \sum_{j=1, j \neq i, q}^{N} m_j \frac{\partial R_{ij}}{\partial \overline{r}_{qi}} \tag{2.45}$$

where m_j is the mass of the disturbing body,

$$R_{ij} = G \left(\frac{1}{r_{ij}} - \frac{\overline{r}_{qi} \cdot \overline{r}_{qj}}{r_{qj}^3} \right) \tag{2.46}$$

The vector $\bar{r}$, which is the vector from the center body to the spacecraft is equal to $\overline{r}_{qi}$. The vector $\overline{r}_{ij}$ is given by:

$$\overline{r}_{ij} = \overline{r}_{qi} - \overline{r}_{qj} \tag{2.47}$$

Ephemeris data are used to obtain $\overline{r}_{qj}$ at any given time. These values are calculated by Copernicus or Turboprop. The gravitational acceleration due to the perturbing masses is given by:

$$\overline{g}(t, \overline{r})_{\text{point masses}} = \overline{\nabla} U_{\text{point masses}}$$
$$= G \sum_{j=1, j \neq i, q}^{N} m_j \left(\frac{\overline{r}_{ij}}{r_{ij}^3} - \frac{\overline{r}_{qj}}{r_{qj}^3} \right) \tag{2.48}$$

The right hand equation has two terms, the first term is a direct perturbing term and second is an indirect perturbing term. As the spacecraft (i) changes its position relative to the central body (q) the direct terms change as well. The indirect terms are not affected under the restricted model assumption, therefore they do not contribute to G_r. Letting $\mu_j = Gm_j$,

$$G_r = \sum_{j=1, j \neq i, q}^{N} \frac{\mu_j}{r_{ij}^5} (3\overline{r}_{ji} r_{ji}^T - r_{ji}^2 I) \tag{2.49}$$

Letting $\overline{r}_{ji} = (x_{ji}\hat{x} + y_{ji}\hat{y} + z_{ji}\hat{z})$.

$$G_{t,r\text{point masses}} = \begin{bmatrix} \sum \frac{\mu_j}{r_{ji}^5}(3x_{ji}^2 - r_{ji}^2) & \sum 3\frac{\mu_j}{r_{ji}^5}x_{ji}y_{ji} & \sum 3\frac{\mu_j}{r_{ji}^5}x_{ji}z_{ji} \\ \sum 3\frac{\mu_j}{r_{ji}^5}x_{ji}y_{ji} & \sum \frac{\mu_j}{r_{ji}^5}(3y_{ji}^2 - r_{ji}^2) & \sum 3\frac{\mu_j}{r_{ji}^5}y_{ji}z_{ji} \\ \sum 3\frac{\mu_j}{r_{ji}^5}x_{ji}z_{ji} & \sum 3\frac{\mu_j}{r_{ji}^5}y_{ji}z_{ji} & \sum \frac{\mu_j}{r_{ji}^5}(3z_{ji}^2 - r_{ji}^2) \end{bmatrix} \tag{2.50}$$

$$G_{v,\text{point masses}} = [0]_3 \tag{2.51}$$

where $\sum = \sum_{j=1 j \neq i,q}^{N}$. Since G_v is equal to zero, then Equation 2.44 is satisfied because $\bar{g}_1$ is only a function of time and position, and Equation 2.41 is satisfied for the same reason. Therefore, when point masses are added the two equations are satisfied and primer vector theory is applicable without further modifications.[6]

2.3   Previous Applications of Primer Vector Theory

Lion and Handelsman extended Lawden's primer vector theory work to include conditions when an additional impulse, initial coasts and/or final coasts can be used to lower the cost of the original non-optimal reference trajectory. The coasts that can be used to improve a trajectory are for time free trajectories, meaning that the total time of the trajectory can vary.[15] Jezewski and Rozendaal developed a technique for determining optimal n-impulse trajectories.[11] Prussing extended primer vector theory into time-fixed cases for orbit to orbit transfers.[20, 21] A technique for optimizing finite thrust transfers and impulsive maneuvers was investigated by Colasurdo and Pastrone.[2]

The previous references were in the two body problem, but primer vector theory has also been applied in the restricted three body problem. The elliptic restricted three body problem was used by Hiday to build optimal transfers between libration point orbits.[7] Davis extended it to the circular restricted three body problem to build optimal trajectories between libration point orbits using invariant manifolds.[3] Primer vector theory has also been used in designing low thrust transfers in circular restricted three body problem by Russell.[18, 22]

Chapter 3

Optimizing Earth to Halo Orbit Trajectories

Earth to halo orbit trajectories were built to examine whether a mid-course maneuver after the powered lunar flyby decreases the total ΔV of the trajectory. If the primer plot indicates that a mid-course maneuver is needed, a MCM was added and the resulting primer plot and cost savings were examined. A MCM was added before the flyby to see if the primer plot still indicates that a later MCM is required. The burn during the lunar flyby was removed in order to see if the primer plot indicates that this burn is beneficial to the trajectory.

3.1   Baseline Trajectory

Each trajectory is made up of four segments, followed by a halo orbit. A pictorial representation of the trajectory and the locations of the maneuvers as shown in Figure 3.1. The trajectory was built using the flight rules for this mission design given in Table 3.1. Segments 3 and 4 each have a one day length constraint to ensure that there is at least a day between each burn for navigation reasons. All of the constraints that were used to create these trajectories in Copernicus are shown in Table 3.2. To ensure that a continuous trajectory was created, if these constraints were not satisfied, the trajectory was not used. A picture of the trajectory from Copernicus is shown in Figure 3.2.
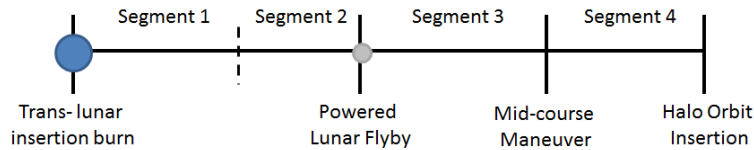
Figure 3.1: Trajectory Design

Table 3.1: Flight Rules for this Mission Design

Total Trajectory Length	= 8 days
Total ΔV	< 600 m/s
Segment 3 length, propagated forwards in time	$\geq$ 1 day
Segment 4 length, propagated backwards in time	$\leq$ -1 day
Radius of Perilune	$\geq$ 1837.4 km

Table 3.2: Constraints Used in Building Earth to Halo Orbit Copernicus Trajectories

Segment 2 Final Position and Velocity = Segment 1 Final Position and Velocity
Segment 2 Final Time = Segment 1 Final Time
Segment 2 Radius of Perigee at Moon $\geq$ 1837.4 km
Segment 3 Final Position and Velocity = Segment 4 Final Position and Velocity
Segment 3 Duration $\geq$ 1 day
Segment 3 MCM Maneuver $\geq$ 20 m/s
Segment 4 Duration $\leq$ -1 day
Total Duration = 8 days
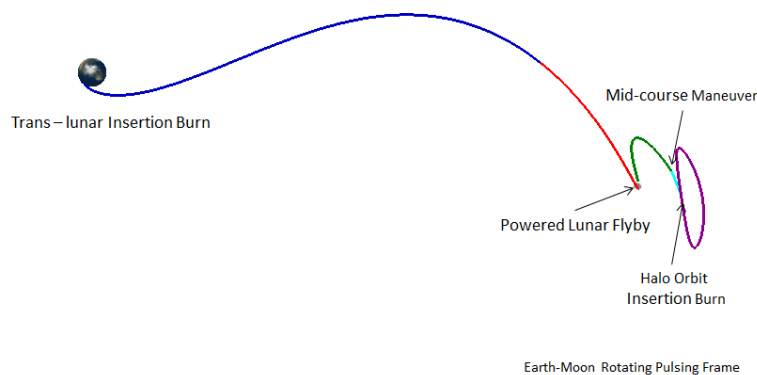
Figure 3.2: Trajectory Design to Earth-Moon L_2 Halo Orbit

3.2   Building Earth to Halo Orbit Trajectories in Copernicus

3.2.1   Segment 1 Definition

The first segment is initialized in low Earth orbit and has an initial impulsive maneuver called the trans-lunar insertion burn, and is propagated forward in time. Its state definition and optimization variables, variables that the built in optimizer SNOPT can alter, are listed in Table 3.3. While there is a reference epoch for this trajectory, the start time does not need to be that day and is allowed to vary. This allows the optimizer to select the best day to perform the trans-lunar insertion burn and have the spacecraft start the trajectory to the halo orbit. This segment propagates forwards in time to approximately the half-way point between the Earth and the Moon.

Table 3.3: Segment 1 State Definition and Optimization Variables

State	Optimization Variable or Value, Earth J2000 Frame
Semi-major axis (km)	6563.14
Eccentricity	0
Inclination (degrees)	28.5
Right Ascension of Ascending Node	OV
Argument of Periapsis (degrees)	0
True Anomaly	OV
T_0 (day)	OV
DT (day)	2.0

3.2.2   Segment 2 Definition

The second segment is initialized at the Moon, with the state definition shown in Table 3.4. It is propagated backward in time from the Moon state to meet up with the end of the first segment. There is a constraint that the radius of perilune has to be greater than 100 km off the surface of the Moon.

Table 3.4: Segment 2 State Definition and Optimization Variables

State	Optimization Variable, Moon J2000 Frame
Incoming V_∞ vector	OV
Right Ascension of V_∞ vector	OV
Declination of V_∞ vector	OV
Right Ascension of Ascending Node	OV
Radius of Perilune	OV
True Anomaly (degrees)	0
T_0 (day)	OV
DT (day)	-1.1

3.2.3   Segment 3 Definition

The third segment is defined at the same Moon state as Segment 2, with an initial maneuver for the powered lunar flyby, and is propagated forward in time. There is a maneuver at the end of Segment 3 for the mid-course maneuver, if it is applicable. The initial time of this segment is the same as the initial time for Segment 2, but the duration of this segment is an optimization variable. This segment is propagated forwards in time to meet up with the end of Segment 4.

3.2.4   Segment 4 Definition

A halo orbit is defined eight days after the epoch with the initial conditions given in Table 3.5. The halo insertion location does not have to be at these initial conditions. The halo orbit is propagated forwards in time in order for the optimizer to select the best location for the insertion into the halo orbit. This segment starts at the halo orbit insertion location and is propagated backwards to meet up with the end of Segment 3.

Table 3.5: Halo Orbit Initial Conditions

State	Value in Earth J2000 Frame
R_x (km)	443,759.676
R_y (km)	-28,353.459
R_z (km)	-58,819.425
V_x (km/s)	0.247
V_y (km/s)	1.038
V_z (km/s)	0.423

3.3   Earth to Halo Orbit Trajectories

Table 3.6 lists all of the trajectories shown in this chapter as well as explaining the changes that were made to create those trajectories. Trajectories will be referred to by number henceforth.

3.3.1   Trajectory with MCM - Trajectory 1

The baseline trajectory was built with the MCM at the end of Segment 3. Using the built-in SNOPT optimizer in Copernicus, the parameters listed in Table 3.3 were allowed to vary in order to create a continuous trajectory. The initial time, which is the number of days after the epoch, and duration of each segment of Trajectory 1 are listed in Table 3.7. Once a continuous trajectory was built, the primer vector of the trajectory was calculated and plotted. Because the primer vector is only defined between two impulsive burns the four segments are shown as three sections. As you can see in Figure 3.3(a), in Trajectory 1, the primer magnitude starts at a value of 1 for each section and remains below 1 for the duration. Figure 3.3 has labels for each event within the trajectory and the following primer plots for other trajectories will have a similar format.

3.3.2   Trajectory without MCM - Trajectory 2

In order to make the same trajectory without the MCM, the time variables of each segment were kept the same and the maneuver at the end of Segment 3 was removed. Copernicus with SNOPT optimized a new geometry to get a continuous trajectory. Once this was done, the primer magnitude was calculated for the entire trajectory and was plotted in Figure 3.3(b). As can be seen in Figure 3.3(b), the primer magnitude in Segment 3 exceeds 1, indicating a need for an additional impulse during that part of the trajectory. The total ΔV's of both reference trajectories are listed in Table 3.8.

Table 3.6: Description of each Earth to Halo Orbit Trajectory

Trajectory Number	Description	Changes made to Previous Trajectory
Trajectory 1	Baseline Trajectory with MCM	N/A
Trajectory 2	Baseline Trajectory without MCM	N/A
Trajectory 3	Added MCM	MCM was added at the primer magnitude peak of Trajectory 2.
Trajectory 4	Added MCM and vary time of MCM	MCM was added to Trajectory 2, and time was allowed to vary.
Trajectory 5	New Trajectory	Allowed time of Trajectory 2 events to change. Removed restriction that Segment 3 and 4 must be 1 day, start time allowed to vary for Segments 1 and 2. Duration of segment 3 and halo orbit insertion location were allowed to vary.
Trajectory 6	New Trajectory	Allowed time of Trajectory 2 events to change, with the 1 day constraint for Segments 3 and 4 still in place. Initial time for Segments 1 and 2, duration of Segment 1, and 2 and halo orbit insertion location were allowed to vary.
Trajectory 7	New Trajectory	Initial time and duration for Segment 1, Segment 2 and halo insertion location were allowed to vary. Segment 3 duration was set to one day.
Trajectory 8	Add MCM to New Trajectory	MCM was added to Trajectory 6.
Trajectory 9	Add MCM to New Trajectory	Larger MCM was added to Trajectory 6.
Trajectory 10	Add MCM before Flyby	MCM before flyby was added to Trajectory 1. Initial time of segment 1 and 2 as well as the duration of Segment 3 and the halo orbit insertion location were allowed to vary.
Trajectory 11	Add MCM before Flyby	MCM before flyby was added to Trajectory 2. Initial time of segment 1 and 2 as well as the duration of Segment 3 and the halo orbit insertion location were allowed to vary.
Trajectory 12	No Powered Lunar Flyby	The powered lunar flyby was removed from Trajectory 1, and optimization variables were unchanged.

3.3.3 Adding MCM Maneuver to Trajectory 2

In order to place a new maneuver into the trajectory in Copernicus, the end time of Segment

3 was set to the time that the maximum primer magnitude occurred in Trajectory 2. The maneuver
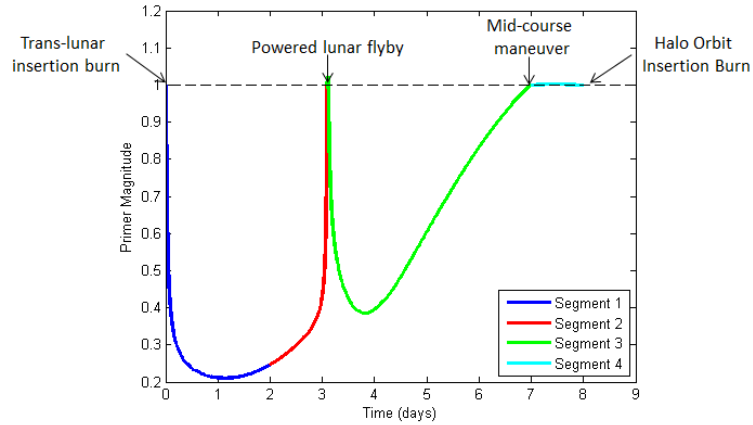
(a) Primer Plot of Trajectory 1
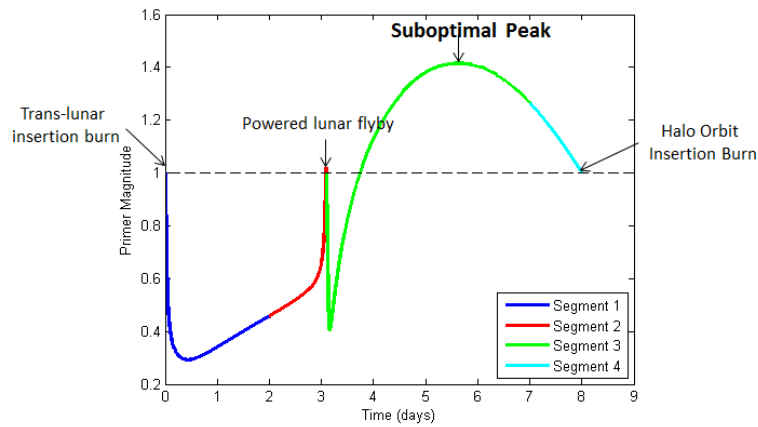
(b) Primer Plot of Trajectory 2

Figure 3.3: Primer Plot of Trajectories 1 and 2

Table 3.7: Initial and Duration Times for Trajectory 1 and 2

Segment	Duration (days)
Segment 1 T_0, days since reference epoch	3.062
Segment 1 Duration	2.0
Segment 2 T_0, days since reference epoch	6.162
Segment 2 Duration	-1.1
Segment 3 T_0, days since reference epoch	6.162
Segment 3 Duration	3.9
Segment 4 T_0, days since reference epoch	11.062
Segment 4 Duration	-1.0

was constrained to be equal to 20 m/s or larger. This was done to ensure that Copernicus inserted

Table 3.8: ΔV Values of Trajectories 1 and 2

| ΔV Type	Trajectory 1 (m/s)	Trajectory 2 (m/s)
Total ΔV	340.949	349.968
Flyby ΔV	221.753	221.071
MCM ΔV	56.589	N/A
HOI ΔV	62.607	128.897

a ΔV instead of leaving the maneuver magnitude at 0, or at a very small number. Once the maneuver was added, Copernicus was allowed to optimize the geometry of the trajectory, but the timing of the trajectory was kept the same. This trajectory will be called Trajectory 3 from now on. Segment 4 slightly exceeds primer magnitude value of 1 as can be seen in Figure 3.4(a), indicating this location of the MCM may not be optimal. Therefore, the time of the MCM was allowed to vary and be selected using the SNOPT optimizer within Copernicus, and this trajectory is called Trajectory 4. Doing this reduced the magnitude of the primer vector to below 1 in Segment 4 as can be seen in Figure 3.4(b). The ΔV values for both of these trajectories are listed in Table 3.9.

Table 3.9: ΔV Values for Trajectories 3 and 4

ΔV Type and Segment Duration	Trajectory 3 (m/s)	Trajectory 4 (m/s)
Total ΔV	343.544	340.995
Cost Savings	6.424	8.973
Flyby ΔV	221.092	221.877
MCM ΔV	30.217	56.876
HOI ΔV	92.235	62.242
Segment 1 Duration(days)	2.0	2.0
Segment 2 Duration (days)	-1.1	-1.1
Segment 3 Duration (days)	2.53	3.9
Segment 4 Duration (days)	-2.37	-1.0

3.4   Building New Earth to Halo Orbit Trajectories

In order to see if these results can be repeated for other trajectories, Trajectory 2 was used and the timing of certain events was changed. First, the one day duration restriction on Segments 3 and 4 was lifted, so the duration of Segment 3 and the halo orbit insertion location were allowed to vary. The initial time of Segments 1 and 2 were also allowed to vary in this trajectory, called
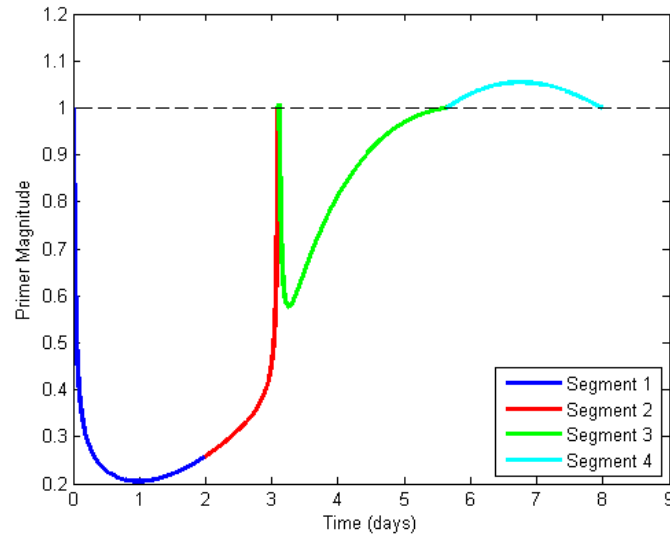
(a) Primer Plot of Trajectory 3
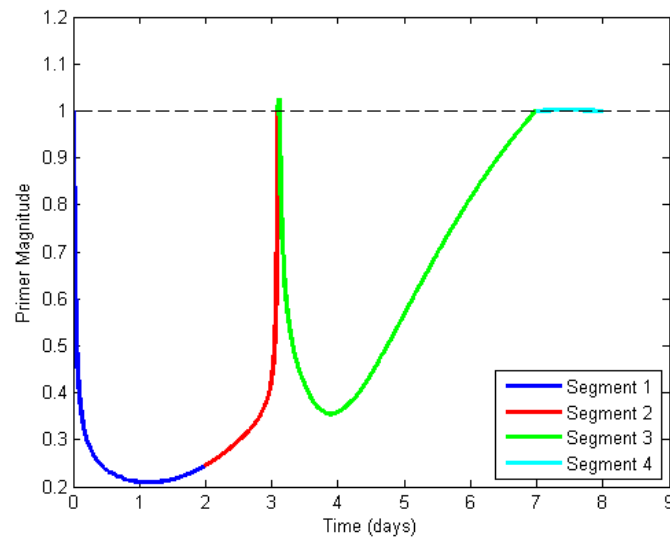
(b) Primer Plot of Trajectory 4

Figure 3.4: Primer Plot of Trajectories 3 and 4

Trajectory 5. The primer vector output is shown in Figure 3.5(a).

To see if allowing additional terms to vary from Trajectory 2 would create a different outcome, the one day duration restriction for Segments 3 and 4 was reinstated and the initial times of Segments 1 and 2, as well as the duration of those segments and the halo orbit insertion location, were allowed to vary. This trajectory is called Trajectory 6 from now on and its primer output is
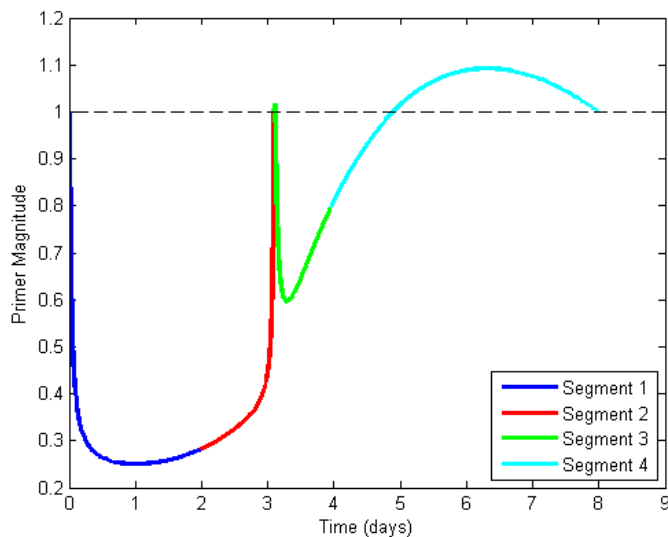
(a) Primer Plot of Trajectory 5
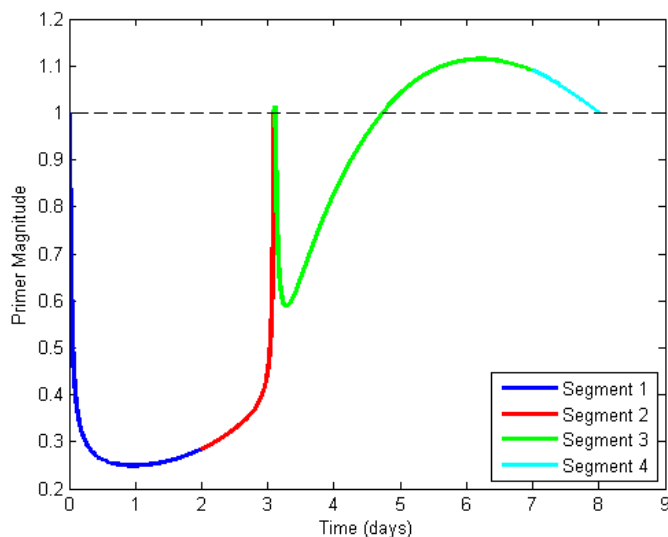
(b) Primer Plot of Trajectory 6

Figure 3.5: Primer Plots of Trajectories 5 and 6

shown in Figure 3.5(b).

A different approach to varying the timing of Trajectory 2 was taken by setting Segment 3's duration to one day and allowing the initial time and duration of Segments 1 and 2 to vary, as well as the halo orbit insertion location, resulting in a new trajectory. This new trajectory, Trajectory 7, has a total ΔV of 280.811 m/s. Examining the primer output in Figure 3.6 shows that there is

no peak in the primer magnitude, therefore a MCM is not needed. This illustrates that there exist trajectories where a MCM is not needed. The peak time and total ΔV for each of these trajectories are listed in Table 3.10.
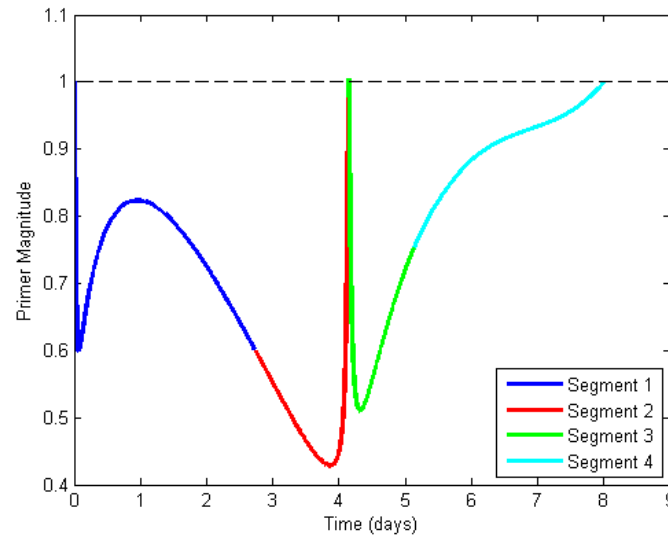
Figure 3.6: Primer Plot of Trajectory 7

Table 3.10: Total ΔV Values, Peak Time and Segment Duration of Trajectories 5, 6 and 7

ΔV Type, Peak Time and Segment Duration	Trajectory 5 (m/s)	Trajectory 6 (m/s)	Trajectory 7 (m/s)
Total ΔV	344.774	344.439	280.811
Flyby ΔV	221.686	220.902	174.291
HOI ΔV	123.088	123.537	106.520
Peak Time (days)	6.31	6.21	N/A
Segment 1 Duration (days)	2.0	2.0	2.72
Segment 2 Duration (days)	-1.1	-1.1	-1.42
Segment 3 Duration (days)	0.85	3.9	1.0
Segment 4 Duration (days)	-4.05	-1	-2.86

3.4.1   Adding MCM to Trajectory 6

A MCM was added to Trajectory 6 to see if this would reduce the total ΔV, resulting in Trajectory 8. The time that the peak of the primer magnitude occurred in Trajectory 6 was used as an initial estimate for the time of the MCM, but this time was allowed to vary. The primer output is shown in Figure 3.7(a), and Segments 3 and 4 both exceed 1 slightly, the maximum values being 1.032 and 1.016 respectively. This shows that perhaps the magnitude of the MCM was not sufficient; however attempts to correct this were not fruitful.

During iterations to get Trajectory 8, a larger peak in Segment 3 was found. Therefore it was estimated that two MCMs might be needed after the powered lunar flyby. The constraint that there must be a day between maneuvers was not enforced. Adding a second MCM did not result in a lower total ΔV trajectory, but it resulted in one interesting case. In this case, the time between the maneuvers was 0.02 days, therefore these segments were combined by making the end of Segment 3 occur at this time, but allowing it to vary, and constraining the maneuver to be 40 m/s or more. This resulted in a new trajectory with a slight decrease in total ΔV. The primer plot of this trajectory, Trajectory 9, is shown in Figure 3.7(b) and ΔV values are in Table 3.11.

Table 3.11: ΔV Value for Trajectories 8 and 9

ΔV Type and Segment Duration	Trajectory 8 (m/s)	Trajectory 9 (m/s)
Total ΔV	342.899	343.105
Cost Savings	1.54	1.334
Flyby ΔV	222.143	225.090
MCM ΔV	20.777	40.0
HOI ΔV	99.979	78.015
Segment 1 Duration (days)	2.0	2.0
Segment 2 Duration (days)	-1.1	-1.1
Segment 3 Duration (days)	2.6	3.9
Segment 4 Duration (days)	-2.3	-1.0
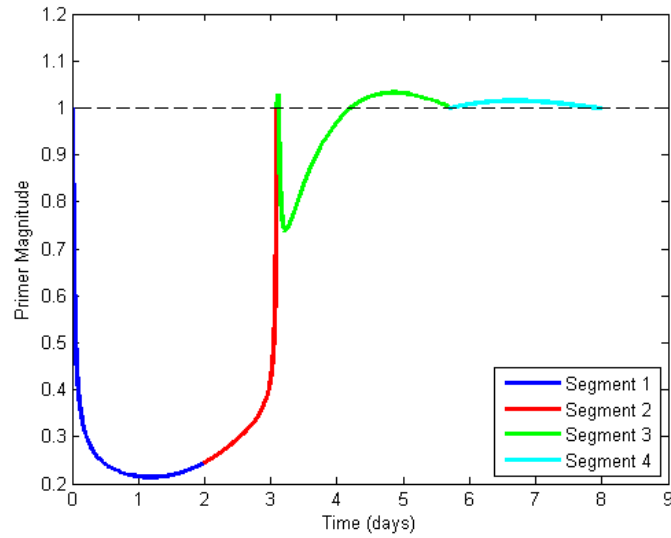
(a) Primer Plot of Trajectory 8
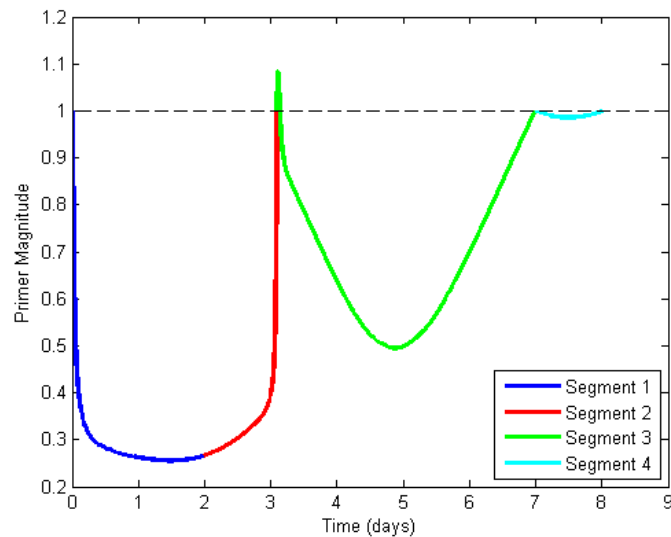
(b) Primer Plot of Trajectory 9

Figure 3.7: Primer Plot of Trajectories 8 and 9

3.5   Investigating Adding Mid-Course Maneuver Before Flyby

A mid-course maneuver was added before the powered lunar flyby in order to test if adding a

MCM in another location would create a better trajectory. The maneuver was added in Copernicus

at the end of Segment 1 to Trajectories 1 and 2. For both of these trajectories the initial time

Table 3.12: ΔV Values for Trajectories with MCM before Flyby

ΔV **Type**	**Trajectory 10 (m/s)**	**Trajectory 11 (m/s)**
Total ΔV	356.073	359.218
MCM before flyby	20.0	20.0
Flyby	216.285	215.495
MCM after flyby	54.25	N/A
Halo Orbit Insertion	65.538	123.722

of Segments 1 and 2, the duration of Segment 3 and the halo insertion location were allowed to vary. First the MCM was constrained to be greater than or equal to 20 m/s. The trajectory that was created using Trajectory 1 is to be called Trajectory 10 and the trajectory that was created from Trajectory 2 is to be called Trajectory 11. Adding this MCM increased the total ΔV in both cases slightly as can be seen in Table 3.12. Also, the ΔV for the new MCM is exactly the required amount of 20 m/s. The primer plot output for Trajectory 10 is shown in Figure 3.8(a), and primer plot for Trajectory 11 is shown in Figure 3.8(b). As you can see from Figure 3.8(b), there is still a peak in primer magnitude, which indicates that an additional maneuver is needed.

Because the value of the MCM before the flyby was at the constrained minimum, that constraint was removed to see which value the SNOPT optimizer in Copernicus would determine. For both trajectories, the optimizer essentially removed the MCM because its magnitude was set equal to zero, demonstrating that this MCM is not needed.

3.6   Non-powered Lunar Flyby Investigation

The approach of investigating if a maneuver is necessary was applied to the powered lunar flyby. Trajectory 1's powered lunar flyby, which is the maneuver at the beginning of Segment 3, was removed and the same optimization variables were used as were used to generate Trajectory 1. The one day constraint on Segments 3 and 4 was left in place. In the resulting trajectory, Trajectory 12, a flyby of the Moon still occurs with the radius of perilune being 1902.89 km. The primer plot of this trajectory is shown in Figure 3.9. As can be seen there is a spike in primer magnitude that occurs where the maneuver was previously located. This demonstrates that there is a need for a
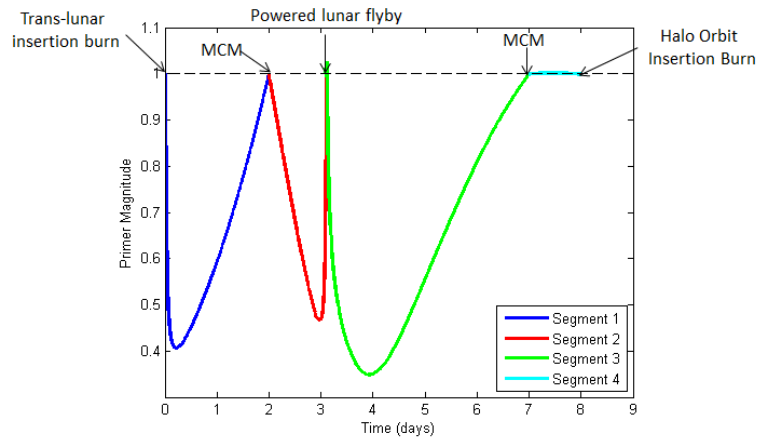
(a) Primer Plot of Trajectory 10
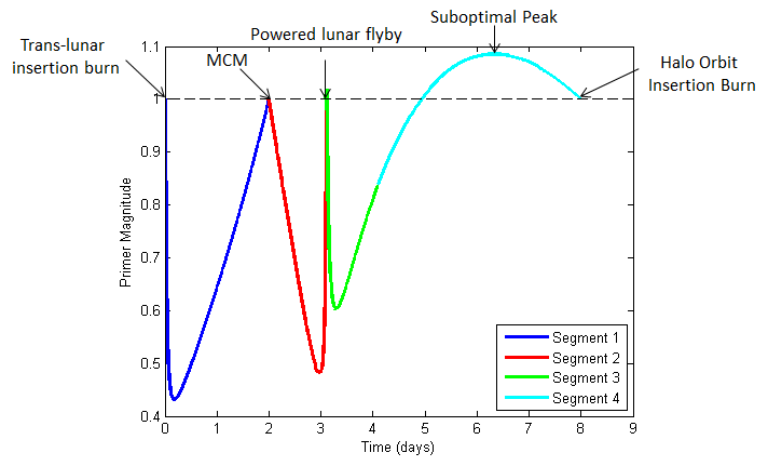
(b) Primer Plot of Trajectory 11

Figure 3.8: Primer Plots of Trajectories 10 and 11

maneuver at that location, especially when the total ΔV's for this trajectory, as seen in Table 3.13, are compared to Trajectory 1. There is a significant increase in total ΔV when there is no powered lunar flyby, which illustrates that adding the powered flyby is beneficial to the trajectory.

Table 3.13: ΔV Values of Trajectory 12

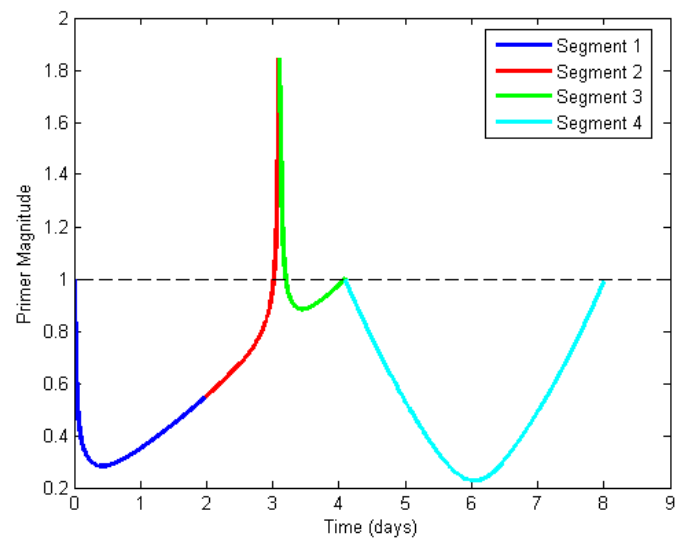| ΔV **Type**	**Trajectory 12**
Total ΔV (m/s)	1181.713
MCM (m/s)	1135.637
HOI (m/s)	46.076

Figure 3.9: Primer Plot of Trajectory 12

Chapter 4

Round Trip Trajectories

Round trip trajectories were built in order to examine where a mid-course maneuver should be added on the outbound and inbound trajectories. These trajectories entered the halo orbit at a specified τ angle, and a variety of τ angles were used to generate diverse trajectories. Three trajectories were chosen to have mid-course maneuvers added when the primer plot indicated that it would be beneficial to the trajectory.

4.1   Building Round Trip Trajectories in Copernicus

Round trip trajectories were built in Copernicus with updated overall constraints for the total trajectory as seen in Table 4.1. The restriction on the duration of the Earth to halo orbit portion was changed from equal to eight days to less than or equal to nine days. These round trip trajectories were built to enter the halo orbit at τ values ranging from $0°$ - $360°$ in 20 degree increments. This was done in order to see if there were trends around the entire orbit and to create diverse trajectories. The Earth to halo orbit parts of these round trip trajectories were built in the same way as before with several constraint changes. The constraint that the duration of Segments 3 and 4 had to be greater than a day was removed. The restriction of one day between burns was relaxed to half a day between burns. This was primarily done since the duration between the halo orbit and Moon on the inbound part of the trajectory tended to be short, generally between 1-1.5 days. In order to allow a burn to be done after exiting the halo orbit and before reaching the Moon, the restriction on the length between burns had to be altered.

Table 4.1: Constraints for Round Trip Trajectory

Earth to Halo Orbit Duration	≤ 9 days
Spacecraft in Halo Orbit Duration	≥ 5 days
Total Duration	≤ 21 days
Total ΔV	≤ 1340 m/s
Halo Orbit to Moon Duration	≥ 1 day
Time Between Burns	≥ 0.5 days

There are nine segments in the round trip trajectories, the first three segments are the same as in the Earth to halo trajectories. Segment 4's initial time was defined by the τ value that it enters the halo orbit at and was not allowed to vary. The fifth segment is when the spacecraft is in the halo orbit. To ensure that a continuous trajectory is created, constraints were used to create the trajectories in Copernicus and are seen in Table 4.2, and if these constraints were not met than the trajectory was not used. A picture from Copernicus of the halo orbit to Earth part of the round trip trajectory is shown in Figure 4.1.

Table 4.2: Constraint Used in Building Round Trip Copernicus Trajectories

Segment 2 Final Position and Velocity = Segment 1 Final Position and Velocity
Segment 2 Final Time = Segment 1 Final Time
Segment 2 Radius of Perilune at Moon ≥ 1837.4 km
Segment 3 Final Position and Velocity = Segment 4 Final Position and Velocity
Segment 1 to 4 Duration ≤ 9 days
Segment 5 Duration ≥ 5 days
Segment 6 and 7 Duration ≥ 1 day
Segment 6 Final Position and Velocity = Segment 7 Final Position and Velocity
Segment 7 Radius of Perilune at Moon ≥ 1837.4 km
Segment 8 Final Position and Velocity = Segment 9 Final Position and Velocity
Total Duration ≤ 21 days
Total $\Delta V \leq 1340$ m/s

4.1.1 Segment 5 Definition

Segment 5 is when the spacecraft is in the halo orbit and its duration had to be greater than or equal to five days. This duration was because a shorter duration in the halo orbit did not allow
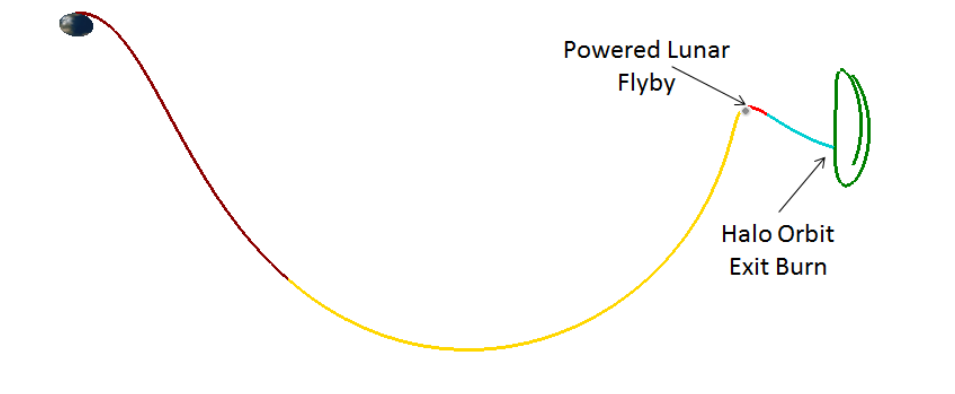
Figure 4.1: Halo Orbit to Earth Trajectory

the astronauts significant time to conduct science missions or tele-operate a rover on the lunar surface. The initial conditions of this segment are the same as Segment 4. There are no maneuvers in this segment, they are performed in Segment 4 and Segment 6.

4.1.2   Segment 6 Definition

This segment is initialized at the final point of Segment 5. There is an initial impulsive maneuver which is used to exit the halo orbit and begin the return to Earth portion of the trajectory. This segment is propagated forwards in time towards the Moon.

4.1.3   Segment 7 Definition

This segment is initialized at the Moon, and is very similar to Segment 2's state definition. The state definition is shown in Table 4.3. There is no maneuver at the Moon state, and the segment is propagated backwards in time to meet up with the end of Segment 6.

4.1.4   Segment 8 Definition

This state is initialized at the same Moon state as Segment 7, but there is an initial impulsive maneuver for the powered lunar flyby. This segment is propagated forwards in time towards

Table 4.3: Segment 7 State Definition and Optimization Variables

State	Optimization Variable, Moon J2000 Frame
Incoming V_∞ vector	OV
Right Ascension of V_∞ vector	OV
Declination of V_∞ vector	OV
Right Ascension of Ascending Node	OV
Radius of Perilune	OV
True Anomaly (degrees)	0
T_0 (day)	OV
DT (day)	OV

Earth.

4.1.5   Segment 9 Definition

This segment was initialized at the Earth using geographic parameters in an ephemeris of
date frame centered on the Earth. The segment is initialized using states in Table 4.4. The altitude
and flight path angle are fixed and the other parameters were allowed to vary. The flight path angle
was the same as used by Pratt et al.[19]

Table 4.4: Segment 9 State Definition and Optimization Variables

State	Optimization Variable, Ephemeris of Date Frame Centered on Earth
Detic Altitude (km)	125
Longitude (degrees)	OV
Detic Latitude (degrees)	OV
Magnitude of the Velocity Vector (km/s)	OV
Centric Azimuth (degrees)	OV
Centric Flight Path Angle (degrees)	-5.8

4.2   Matlab Implementation

Once these round trip trajectories were built, instead of using Matlab and Turboprop to create
the primer vector plots, the trajectories were recreated in Matlab. The segments initial conditions

were held constant, but the ΔV that were applied were allowed to vary using the optimizer fmincon in order to get a continuous trajectory. This was done to make adding mid-course maneuvers into the trajectory and performing primer vector calculations easier and more streamlined. Instead of adding a mid-course maneuver into Copernicus, the maneuver was added in Matlab. Then, like before, the MCM and ΔV's are allowed to vary.

The primer vector plots of the round trip trajectories were built using the ΔV's outlined in the total ΔV equation, Equation 1.1. In order to see what the primer plot looked like after the second powered lunar flyby, the Earth entry velocity condition, which is in the initial velocity of Segment 9, was given the opposite sign and used as a ΔV. This ΔV is referred to as the Fake ΔV at Earth. This was done for illustrative purposes, and no mid-course maneuvers were added in the Moon to Earth segment, even if the primer magnitude exceeded one in this region. An example of what a primer plot of a round trip trajectory looks like is shown in Figure 4.2.
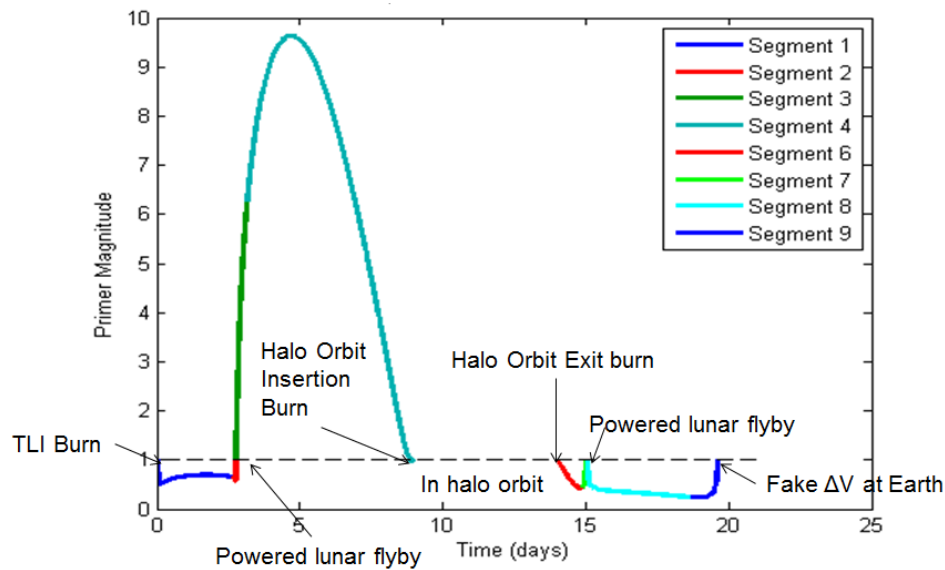

Figure 4.2: $\tau = 60°$ Round Trip Trajectory Primer Plot with ΔV Description

4.3   Applying Primer Vector Theory to Round-Trip Trajectories

Three cases were selected to investigate whether adding a mid-course maneuver was beneficial. These trajectories enter the halo orbit at a τ value of 0, 60 and 200 degrees. Multiple methods were used to investigate the best way to place a maneuver to achieve maximum cost savings. The MCM was always added at the end of a segment. For example, if the primer magnitude peak occurred in Segment 4 the duration of Segment 3 was increased to include the time that the maximum peak occurred. Then the MCM was added at the end of Segment 3.

4.3.1   Description of Methods used to add Mid-Course Maneuver

A mid-course maneuver was first added at the location that primer that primer vector theory calculated as a good initial estimate for the location of the additional impulse in the first method. The method for finding this location is described in Chapter 2.2. While this location can be used as an estimate of the location of the MCM, it is not necessarily the best location. The primer plot will need to be examined in order to see if the time and location of the MCM should be changed.

The next method used was to add the mid-course maneuver at the time that the maximum primer magnitude occurred. This time and the segments' initial conditions that the MCM was being added in were also fixed, unlike the Earth to halo orbit trajectories.

The final method was to allow the optimizer to select the time of the mid-course maneuver. Initially the time of the mid-course maneuver was set to the time that the maximum primer magnitude occurred, but this time was allowed to vary. The half day between burn duration restriction was used to limit when the MCM could occur. If the time that the maximum primer magnitude occurred violated the half day between maneuvers limit, then a half day duration was used. In order to see if other times could generate more cost savings, the time of the MCM was initialized generally at a duration of 1 day or half a day before the next burn. These values were changed based on the output of the primer plot.

4.3.2 $\tau = 60°$ Case

This trajectory entered the halo orbit at a τ angle of 60 degrees. A picture of the trajectory in Copernicus is shown below in Figure 4.3.2. A summary of the trajectory is in Table 4.5.
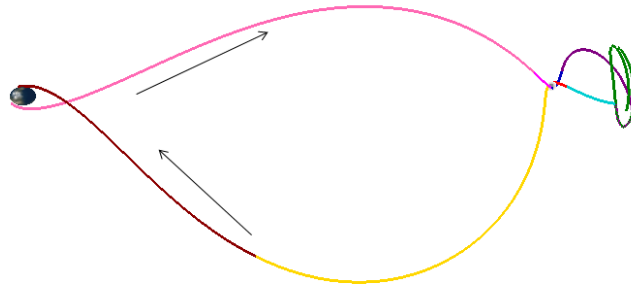

Figure 4.3: $\tau = 60°$ Round Trip Trajectory Picture in Earth-Moon Rotating Frame

Table 4.5: $\tau = 60°$ Trajectory Details

Segment/Parameter	Value
Segment 1 Duration (days)	2.65
Segment 2 Duration (days)	-0.14
Radius of Perilune at Segment 2 (km)	1849.97
Segment 3 Duration (days)	0.39
Segment 4 Duration (days)	-5.82
Segment 1 to 4 Duration (days)	9
Segment 5 Duration (days)	5.0
Segment 6 Duration (days)	0.90
Segment 7 Duration (days)	-0.13
Segment 6 and 7 Duration (days)	1.03
Radius of Perilune at Segment 7 (km)	2072.91
Segment 8 Duration (days)	3.64
Segment 9 Duration (days)	-0.95
Total Trajectory Duration (days)	19.62
Total Trajectory ΔV (m/s)	1045.353
Outbound Flyby ΔV (m/s)	310.287
HOI ΔV (m/s)	152.160
HOE ΔV (m/s)	441.317
Inbound Flyby ΔV (m/s)	141.589

The primer plot of this trajectory is shown in Figure 4.4. Segment 5 was not plotted as there

was a spike in the segment. The spacecraft would not perform the maneuver and would remain in the halo orbit, so this was omitted.
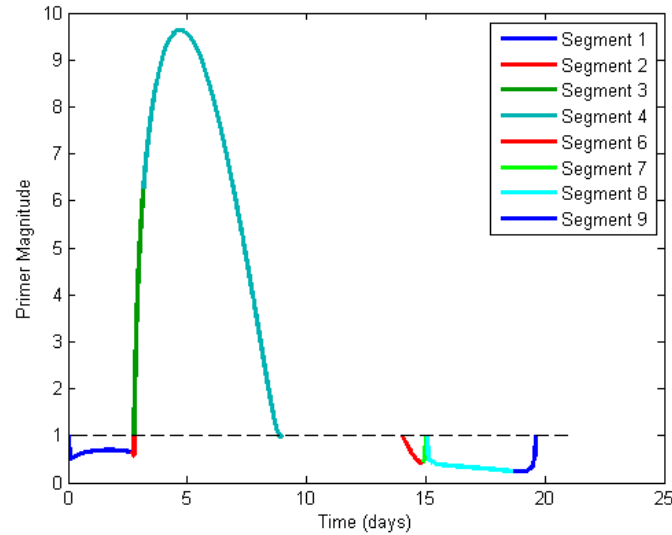

Figure 4.4: $\tau = 60°$ Trajectory Primer Plot

As can be seen in the primer plot, there is only one area where the primer magnitude exceeds 1, and the peak occurs in Segment 4. Therefore, adding an additional impulse in between the moon and halo orbit can reduce the overall cost of the trajectory. First the duration of Segment 3 was changed so that the maximum primer magnitude occurred during Segment 3, which would make it easier to add the mid-course maneuver at the end of the segment.

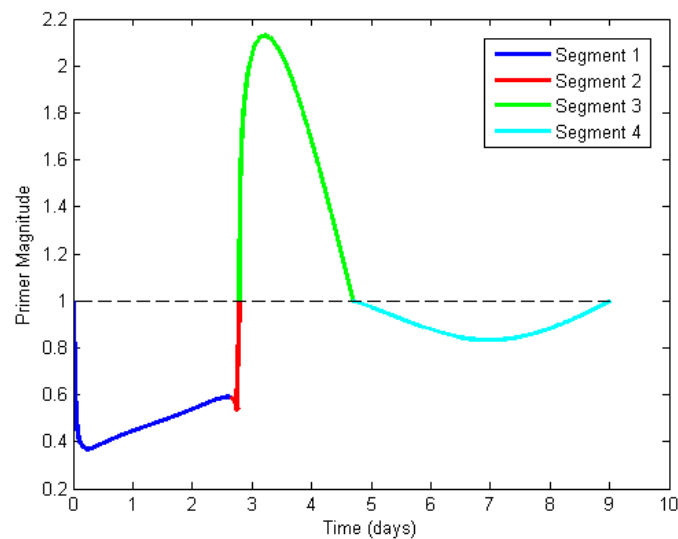### 4.3.2.1   Adding MCM at PVT Calculated Location for $\tau = 60°$ Case

The calculations outlined in Section 2.2 were done to see where primer vector theory suggests the mid-course maneuver should be placed and what the magnitude of the MCM should be. The calculations from primer vector theory are shown in Table 4.6 and the location values are in the Earth J2000 system.

The location of the MCM was fixed at the location calculated from the change in location stated in Table 4.6 and Segments 3 and 4 had to both end at this location. A continuous trajectory

Table 4.6: Primer Vector Theory Calculations for Location of MCM for $\tau = 60°$

PVT Calculation	Value
Calculated Cost Savings (m/s)	1.63
Calculated MCM ΔV (m/s)	0.377
Calculated Change in Location of MCM (km)	[-162.843, 77.992, -157.861]

was found, however, there were no cost savings, in fact the total cost for Segments 3 and 4 increased by 34 cm/s. Therefore, for this case, the PVT calculations for the MCM did not give a good location and magnitude of the MCM. The primer magnitude plot of placing the MCM at this location is shown in Figure 4.5. As can be seen, adding this mid-course maneuver did not completely remove the spike in primer magnitude. As a result, a MCM at this location is not optimal.

Figure 4.5: Primer Plot of MCM Added at Primer Vector Theory Calculated Location for $\tau = 60°$

4.3.2.2   Adding MCM at Maximum Primer Magnitude Time for $\tau = 60°$ Case

Next the MCM was added at the time of the maximum primer magnitude shown in Figure 4.4. Segment 3's duration was changed so that it ended at the time the maximum primer magnitude occurred. The end of Segment 3 was fixed at that time, the mid-course maneuver was added and its magnitude was allowed to vary. Doing this gave a cost savings of 15.92 m/s with a mid-course

maneuver magnitude of 12.36 m/s as shown in Table 4.7. The resulting primer plot is shown in Figure 4.6.

Table 4.7: MCM Added at Maximum Primer Magnitude Time Details for $\tau = 60°$

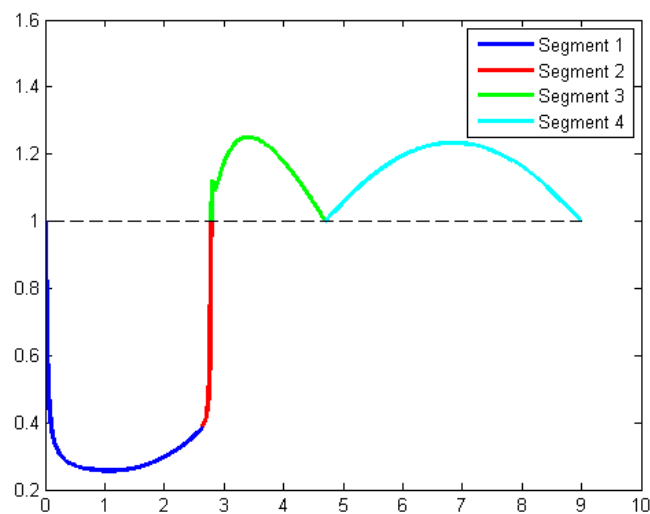| ΔV Type and Segment Duration	Value
Cost Savings (m/s)	15.92
MCM ΔV (m/s)	12.355
Segment 3 Duration (days)	1.91

Figure 4.6: Primer Plot of MCM Added at Maximum Primer Magnitude Time for $\tau = 60°$

While adding this mid-course maneuver generated good cost savings, the primer plot still indicates that there could be a more optimal location for the mid-course maneuver.

4.3.2.3   Optimizer Calculates Time of MCM for $\tau = 60°$ Case

The next method allowed the time that the mid-course maneuver occurred to vary, meaning the duration of Segment 3 varied and the magnitude of the MCM also varied. Giving the optimizer an initial condition of the time that the maximum primer magnitude occurred generated nearly identical solutions with the same primer plots. Next, the duration of Segment 3 was set to 1 day and was allowed to vary. The end result had a Segment 3 duration of 0.69 days and a cost savings

of 18.85 m/s, as can be seen in Table 4.8. The primer plot is shown in Figure 4.7.

Table 4.8: Optimizer Calculates Time of MCM, Segment 3 Duration Initialized at 1 Day Details for $\tau = 60°$

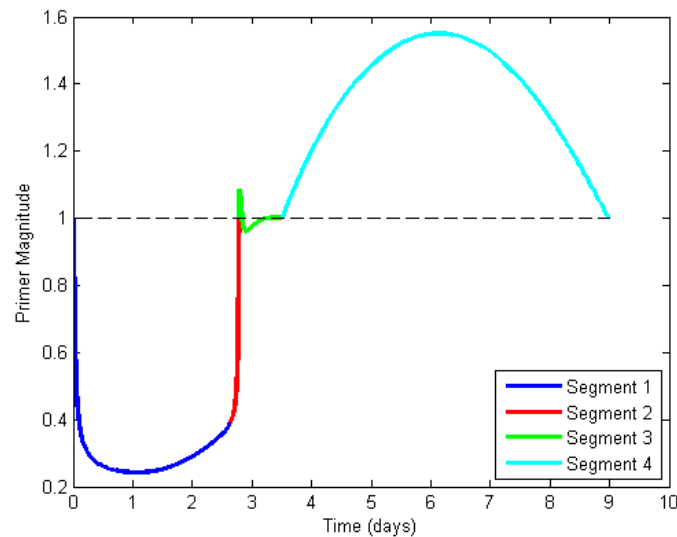| ΔV **Type and Segment Duration**	**Value**
Cost Savings (m/s)	18.85
MCM ΔV (m/s)	15.597
Segment 3 Duration (days)	0.69

Figure 4.7: Primer Plot of Optimizer Calculates Time of MCM, Segment 3 Duration Initialized at 1 Day for $\tau = 60°$

As can be seen from the figure, there is still a spike in the primer magnitude that occurs after the MCM. Therefore, the duration of Segment 3 was initialized to one day before the halo orbit insertion state, which has a duration of 5.21 days. This case did not generate as large cost savings; the duration of Segment 3 ended up being 4.03 days with a cost saving of 4.629 m/s as shown in Table 4.9. The resulting primer plot is shown in Figure 4.8.

Both of these cases have a spike in the primer magnitude despite having a mid-course maneuver and cost savings. Therefore, two mid-course maneuvers were tried since the duration between the Moon and halo orbit was over 6 days and two MCMs would fit in these segments. The first case of Segment 3 duration of 0.698 days was used since it had the greatest cost savings, and a second

Table 4.9: Optimizer Calculates Time of MCM, Segment 3 Duration Initialized to 1 Day Before Halo Orbit for $\tau = 60°$

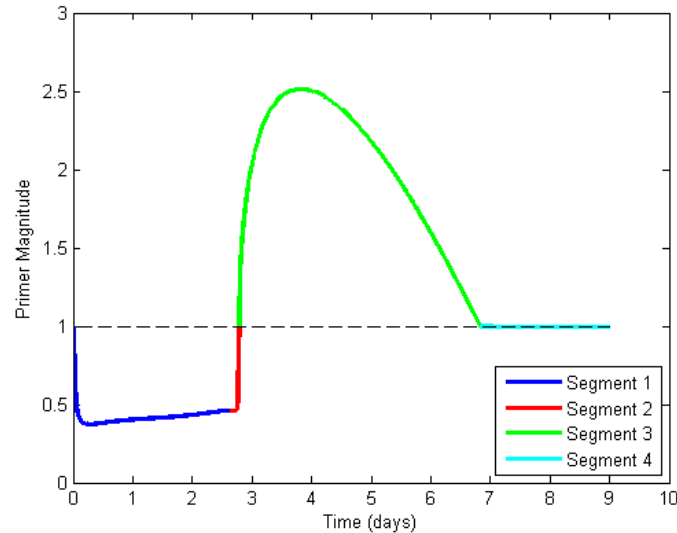| ΔV Type and Segment Duration	Value
Cost Savings (m/s)	4.629
MCM ΔV (m/s)	9.234
Segment 3 Duration (days)	4.03

Figure 4.8: Primer Plot of Optimizer Calculates Time of MCM, Segment 3 Duration Initialized 1 Day before HOI for $\tau = 60°$

MCM was added in Segment 4. The optimizer was not able to find a solution that decreased the total ΔV in Segment 4 of the HOI burn and MCM, and the total ΔV was increased by 5.13 cm/s as shown in Table 4.10. This seems to be a case where PVT is indicates a cost savings could occur but it might be so small that the solver is not picking up on it. Adding this second maneuver in Segment 4 removed the peak that had occurred before as can be seen in Figure 4.9.

Table 4.10: Second MCM Added to Segment 4 Details for $\tau = 60°$

ΔV Type and Segment Duration	Value
Cost Savings (m/s)	-0.0513
MCM ΔV (m/s)	0.0542
New Segment Duration (days)	2.43

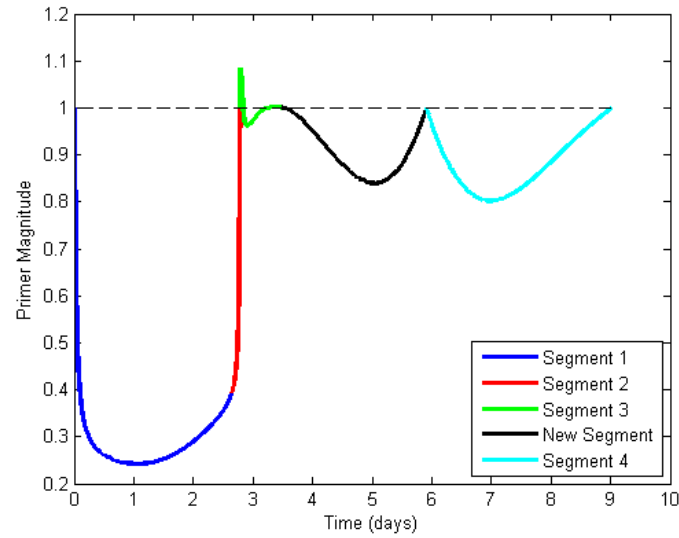Since adding a second MCM did not decrease the total cost, the second MCM is not included.

Figure 4.9: Primer Plot of Second MCM Added to Segment 4 for $\tau = 60°$

Therefore the only MCM that is added is at a Segment 3 duration of 0.69 days. The final cost savings and MCM magnitude is shown in Table 4.11.

Table 4.11: Final Cost Savings for $\tau = 60°$ Case

Final Cost Savings and ΔV	Value
Final Cost Savings (m/s)	18.85
Final MCM ΔV (m/s)	15.597

4.3.3 $\tau = 0°$ Case

This trajectory entered the halo orbit at a τ angle of zero degrees. The total trajectory primer vector plot is shown in Figure 4.10. The plot indicates that an additional impulse in Segments 3 and 7 could reduce the total cost of the trajectory. A summary of this trajectory is given in Table 4.12.

The primer vector theory calculations for the location and magnitude of the additional maneuver for Segment 3 were done and the results are in Table 4.13.
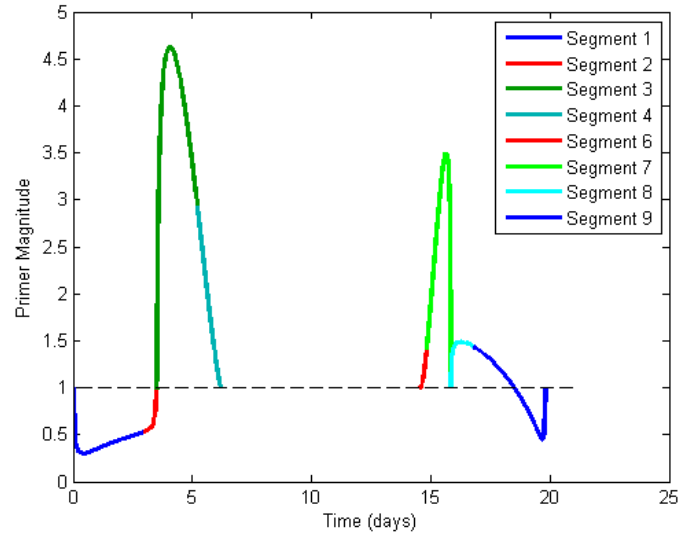
Figure 4.10: $\tau = 0°$ Trajectory Primer Plot

Table 4.12: $\tau = 0°$ Trajectory Details

Segment/Parameter	Value
Segment 1 Duration (days)	2.97
Segment 2 Duration (days)	-0.54
Radius of Perilune for Segment 2 (km)	1837.40
Segment 3 Duration (days)	1.70
Segment 4 Duration (days)	-1.01
Segment 1 to 4 Duration (days)	6.21
Segment 5 Duration (days)	8.36
Segment 6 Duration (days)	0.27
Segment 7 Duration (days)	-1.00
Segment 6 and 7 Duration(days)	1.27
Radius of Perilune at Segment 7 (km)	1849.47
Segment 8 Duration (days)	0.94
Segment 9 Duration (days)	-3.04
Total Trajectory Duration (days)	19.82
Total Trajectory ΔV (m/s)	905.638
Outbound Flyby ΔV (m/s)	190.354
HOI ΔV (m/s)	149.275
HOE ΔV (m/s)	384.714
Inbound Flyby ΔV (m/s)	181.295

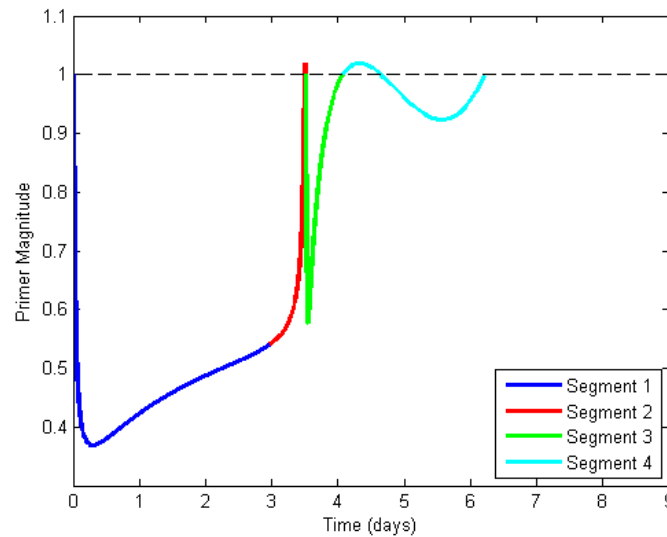### 4.3.3.1   Adding MCM at PVT Calculated Location in Segment 3 for $\tau = 0°$ Case

The MCM was placed at the position given in Table 4.13 and the flyby ΔV and halo orbit

insertion ΔV were varied to meet at that point. A continuous trajectory to this location was found,

Table 4.13: Primer Vector Theory Calculations for Location of MCM in Segment 3 for $\tau=0°$

PVT Calculation	Value
Calculated Cost Savings (m/s)	0.0318
Calculated MCM ΔV (m/s)	0.018
Calculated Change in MCM Location (km)	[-3.409, 7.291, -14.342]

however there was no cost savings. The total cost for Segments 3 and 4 increased by 4.762 cm/s. The primer plot of this is shown in Figure 4.11. There is still a small peak in Segment 4 indicating that a better location of the MCM exists.

Figure 4.11: Primer Plot of MCM Added at Primer Vector Theory Calculated Location in Segment 3 for $\tau=0°$

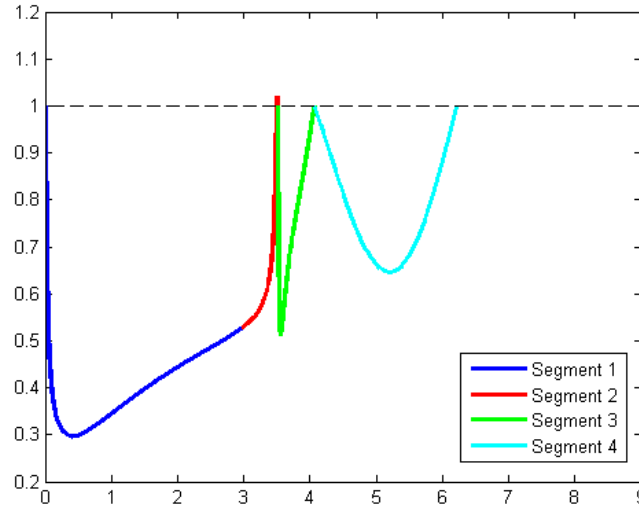### 4.3.3.2 Adding MCM at Maximum Primer Magnitude Time in Segment 3 for $\tau = 0°$ Case

The MCM was next added when the maximum primer magnitude occurred in Figure 4.10 in Segment 3. Having the MCM at this location resulted in 7.438 cm/s cost savings. The primer plot and details of the MCM and cost savings are shown in Figure 4.12 and Table 4.14.

The primer plot indicates that this is a good location for the MCM and primer magnitude

Table 4.14: MCM Added at Maximum Primer Magnitude Time Details for $\tau = 0°$

ΔV **Type and Segment Duration**	**Value**
Cost Savings (m/s)	0.0744
MCM ΔV (m/s)	0.0098
Segment 3 Duration (days)	0.56

Figure 4.12: Primer Plot of MCM Added at Maximum Primer Magnitude Time for $\tau = 0°$

does not exceed one anymore. However the location of the MCM was varied in order to see if a better solution exists.

4.3.3.3 Optimizer Calculates Location of MCM for Segment 3 in $\tau = 0°$ Case

The duration of Segment 3 was set to 1.75 days, but the time was allowed to vary in order for the optimizer to find a good location for the MCM. The final cost savings shown in Table 4.15 was 11.461 cm/s and the duration of Segment 3 was 1.77 days and the primer plot is shown in Figure 4.13. This illustrates that while a good location of the MCM can be found using PVT, a better solution could exist.

Next adding a MCM in Segment 6 and 7 was examined. In order to add a MCM at the end of Segment 6, the duration of Segment 6 was changed such that the maximum primer magnitude

Table 4.15: Optimizer Calculates Time of MCM, Segment 3 Duration Initialized at 1.75 Days for $\tau = 0°$

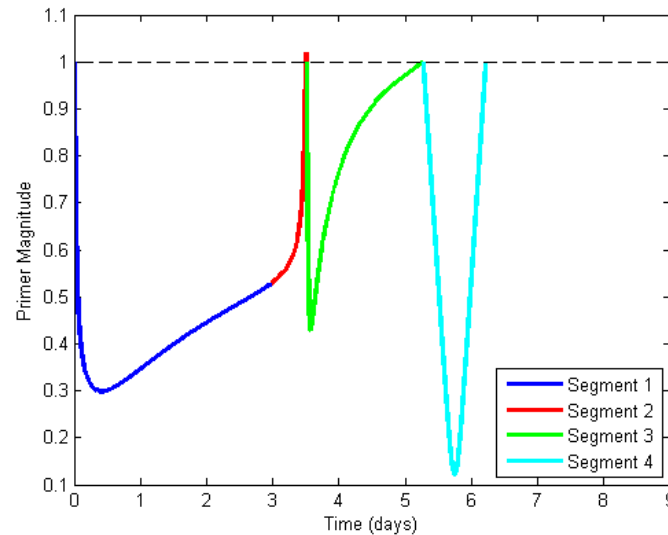| ΔV Type and Segment Duration	Value
Cost Savings (m/s)	0.1146
MCM ΔV (m/s)	0.0005
Duration of Segment 3 (days)	1.77

Figure 4.13: Primer Plot of Optimizer Calculates Time of MCM, Segment 3 Duration Initialized at 1.75 Days for $\tau = 0°$

occurred during Segment 6 instead of Segment 7. The primer vector calculations were done on the new Segment 6 to find where PVT suggests that the MCM should be located. The results of those calculations are in Table 4.16.

Table 4.16: Primer Vector Theory Calculations for Location of MCM in Segment 6 for $\tau = 0°$

PVT Calculation	Value
Calculated Cost Savings (m/s)	11.722
Calculated MCM ΔV (m/s)	14.443
Calculated Change in MCM Location (km)	[-1318.649, 3048.903, -686.881]

Due to the large change in MCM location, a continuous trajectory with Segments 6 and 7 reaching this MCM location was not found. Therefore this technique of finding location of MCM using primer vector theory does not seem to be useful when the difference in location is so large.

4.3.3.4 Adding MCM at Maximum Primer Magnitude Time in Segment 7 for $\tau = 0°$ Case

The MCM was added where the maximum primer magnitude occurred, which had been shifted to occur in Segment 6. This placement violates the half day between burns rule because the length of Segment 7 is 0.185 days. Adding the MCM at this time did not result in cost savings; in fact the cost increased by 0.0613 cm/s, as can be seen in Table 4.17. However the primer plot shows that adding this MCM did remove the peak in primer magnitude as seen in Figure 4.14.

Table 4.17: MCM Added at Maximum Primer Magnitude Location in Segment 6 for $\tau = 0°$

ΔV Type and Segment Duration	Value
Cost Savings (m/s)	-0.000613
MCM ΔV (m/s)	0.00029
Segment 7 Duration (days)	0.185
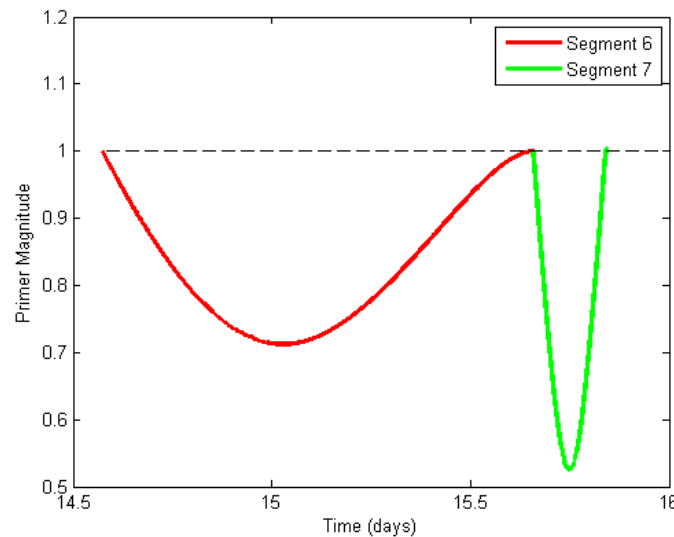
Figure 4.14: Primer Plot of MCM added at Maximum Primer Magnitude Location

4.3.3.5 Optimizer Calculates Location of MCM of Segment 6 for $\tau = 0°$ Case

Segment 6's duration was allowed to vary with the bounds of half day between burns in place. This resulted in a solution with a half day duration for Segment 6 and 4.94 cm/s savings; details

are shown in Table 4.18. The primer plot output shown in Figure 4.15 shows that there is still a peak in primer magnitude with this MCM included, but it is very close to the halo orbit insertion burn.

Table 4.18: Optimizer Calculates Time of MCM in Segment 6 Details for $\tau = 0°$

ΔV **Type and Segment Duration**	**Value**
Cost Savings (m/s)	0.0494
MCM Magnitude (m/s)	0.00106
Segment 6 Duration (days)	0.5
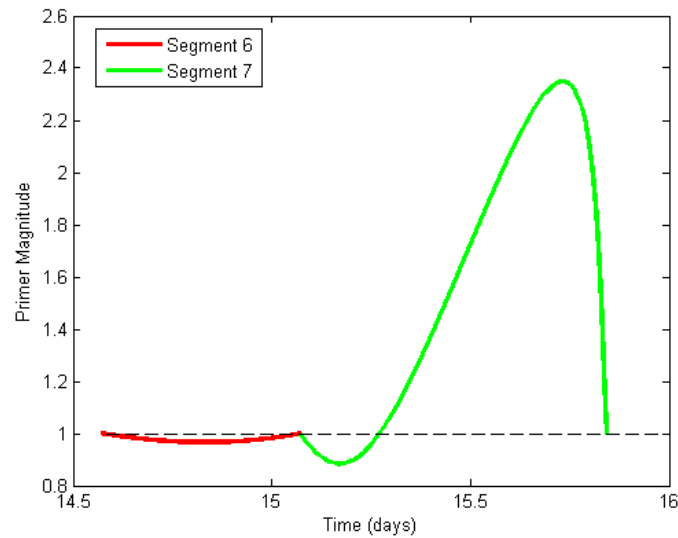
Figure 4.15: Primer Plot of Optimizer Calculates Time of MCM in Segment 6 for $\tau = 0°$

Moving the MCM closer to the halo orbit insertion burn did not increase the cost savings or remove the primer magnitude peak. This indicates that the best location of additional impulse is too close to the halo orbit insertion burn and violates the constraints built in to the trajectory.

4.3.4 $\tau = 200°$ Case

The final case has the spacecraft enter the halo orbit at a τ angle of 200 degrees. The details of this trajectory are given in Table 4.20. The entire trajectory primer plot is given in Figure 4.16. Segment 5 is plotted because it does not have a peak in primer magnitude, so it does not distract

Table 4.19: Final Cost Savings for $\tau = 0°$

Final Cost Savings and ΔV	Value
Final Cost Savings in Segment 3 and 4 (m/s)	0.1146
Final MCM ΔV in Segment 3 (m/s)	0.0005
Final Cost Savings in Segment 6 and 7 (m/s)	0.0494
Final MCM ΔV in Segment 6 (m/s)	0.00106

from the overall primer plot.

Table 4.20: $\tau = 200°$ Trajectory Details

Segment 1 Duration (days)	0.63
Segment 2 Duration (days)	-2.88
Radius of Perilune at Segment 2 (km)	2389.489
Segment 3 Duration (days)	0.50
Segment 4 Duration (days)	-2.42
Segments 1 to 4 Duration (days)	6.43
Segment 5 Duration (days)	5.02
Segment 6 Duration (days)	0.65
Segment 7 Duration (days)	-0.75
Radius of Perilune at Segment 7 (km)	2519.131
Segments 6 and 7 Duration (days)	1.40
Segment 8 Duration (days)	2.37
Segment 9 Duration (days)	-1.07
Total Trajectory Duration (days)	16.445
Total Trajectory ΔV (m/s)	972
Outbound Flyby ΔV (m/s)	276.963
HOI ΔV (m/s)	130.190
HOE ΔV (m/s)	389.435
Inbound Flyby ΔV (m/s)	175.561

The primer plot indicates that a mid-course maneuver can be beneficial in Segments 2 and 3. First, adding an additional impulse in Segment 2 is investigated. As before, the duration of Segment 1 is extended to include the time where the maximum primer magnitude is located so that the MCM can be easily added at the end of Segment 1. The total ΔV used when adding a MCM to Segment 1 was the trans-lunar insertion burn. While this burn is not performed by the Orion, if cost savings could be found then this would be beneficial to the total launch costs, because less fuel would have to be launched.
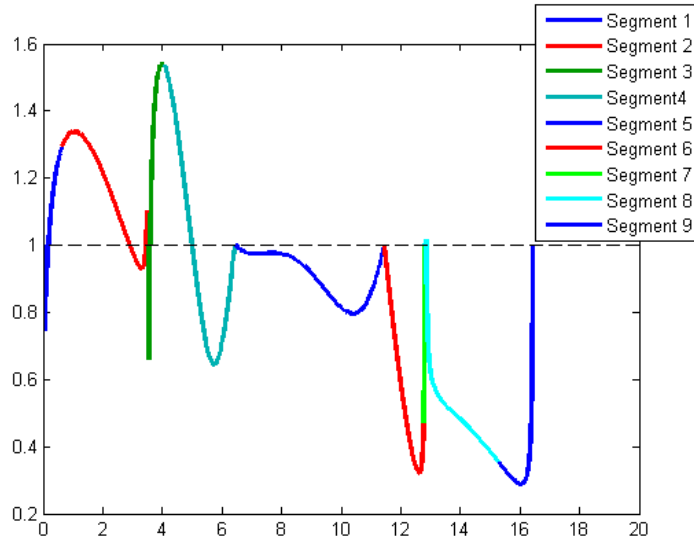
Figure 4.16: $\tau = 200°$ Trajectory Primer Plot

4.3.4.1   Adding MCM at PVT Calculated Location in Segment 1 for $\tau = 200°$ Case

The calculations for the location of the MCM in Segment 1 were done using primer vector theory and the results are in Table 4.21.

Table 4.21: Primer Vector Theory Calculations for Location of MCM in Segment 1 for $\tau = 200°$

PVT Calculation	Value
Calculated Cost Savings (m/s)	0.0286
Calculated MCM ΔV (m/s)	0.169
Calculated Change in MCM Location (km)	[23.561, 21.673, 52.855]

Attempts to add the MCM at this location and have Segments 1 and 2 meet up at that location did not result in a continuous trajectory. Therefore, the change in MCM location was again too great to be used, and the MCM could not be placed at that location.

4.3.4.2   Adding MCM at Maximum Primer Magnitude Time in Segment 1 for $\tau = 200°$ Case

Adding the MCM at the time that the maximum primer magnitude occurred did not lead to cost savings, it increased cost by 0.04 cm/s as can be seen in Table 4.22. The primer plot has a

spike at end of Segment 2 as can be seen in Figure 4.17.

Table 4.22: MCM Added at Maximum Primer Magnitude Time in Segment 1 for $\tau = 200°$

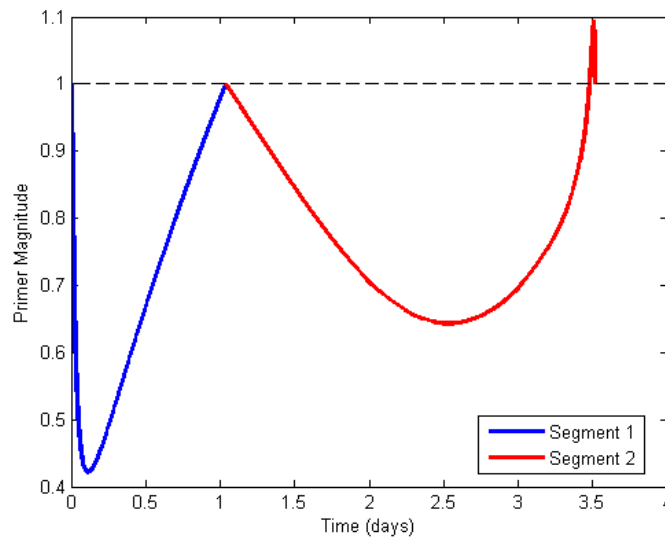| ΔV Type and Segment Duration	Value
Cost Savings (m/s)	-0.0004
MCM Value (m/s)	5.15e-7
Segment 1 Duration (days)	1.04

Figure 4.17: Primer Plot of MCM at Maximum Primer Magnitude Time in Segment 1 for $\tau = 200°$

4.3.4.3   Optimizer Calculates Location of MCM for $\tau = 200°$ Case

Half of the total duration of Segment 1 and 2 was used as an initial guess for Segment 1's duration. This yielded some cost savings as seen in Table 4.23. The primer plot of this new trajectory is seen in Figure 4.18.

Table 4.23: Optimizer Calculate Location of MCM in Segment 1 for $\tau = 200°$

ΔV Type and Segment Duration	Value
Cost Savings (m/s)	0.00189
MCM ΔV (m/s)	4.28e-6
Segment 1 Duration (days)	1.76
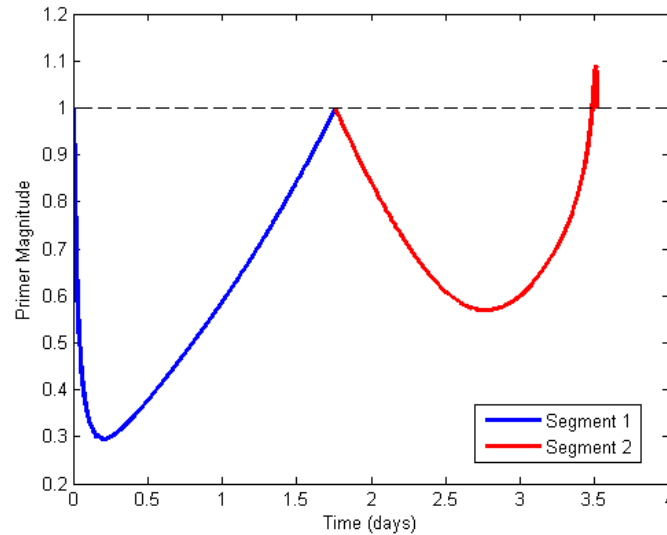
Figure 4.18: Primer Plot of Optimizer Calculate Location of MCM in Segment 1 for $\tau = 200°$

The primer plot has a small spike very close to the powered lunar flyby. Therefore, the next was try to add the MCM closer to the powered lunar flyby. The initial condition used for Segment 1's duration is a half day before the powered lunar flyby. This resulted in slightly higher cost savings, as can be seen in Table 4.24, but there is now a peak in primer magnitude in Segment 1 as can be seen in Figure 4.19.

Table 4.24: Optimizer Calculates Time of MCM, Segment 1 Duration Initialized 0.5 Days before Flyby for $\tau = 200°$

ΔV Type and Segment Duration	Value
Cost Saving (m/s)	0.00236
MCM ΔV (m/s)	7.15e-7
Segment 1 Duration (days)	3.02

Further attempts to remove all peaks in the primer plot did not lead to a continuous trajectory. Therefore, the first case was selected to move forward to adding MCM in Segment 3, due to the fact that the peak in primer magnitude is so close to the powered lunar flyby that there is no way to remedy it. Next, the calculations for the placement and magnitude of the additional impulse using primer vector theory was done for Segment 3 and is shown in Table 4.25.
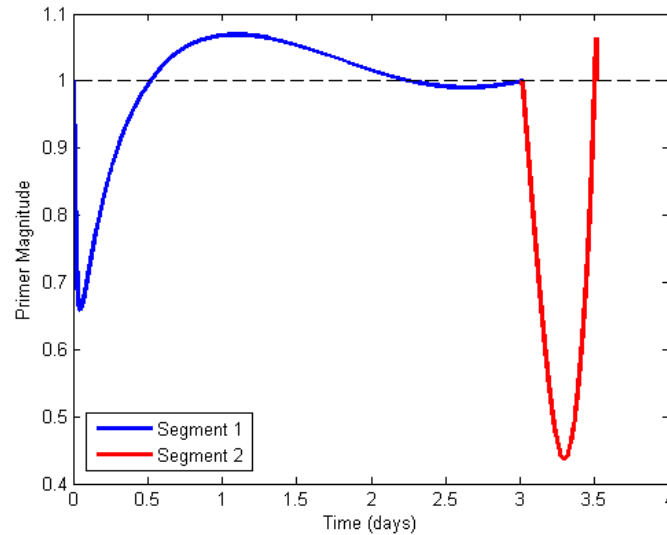
Figure 4.19: Primer Plot of Optimizer Calculate Time of MCM, Segment 1 Duration Initialized 0.5 Days before Flyby for $\tau = 200°$

4.3.4.4   Adding MCM at PVT Calculated Location in Segment 3 for τ=200° Case

Table 4.25: Primer Vector Calculations for Location of MCM in Segment 3 for $\tau = 200°$

PVT Calculation	Value
Calculated Cost Savings (m/s)	0.0145
Calculated MCM ΔV (m/s)	0.054
Calculated Change in MCM Location (km)	[-0.803, 9.307, -10.692]

Using the new location of the MCM found using the change in MCM location in Table 4.25, a continuous trajectory was found but it did not yield any cost savings. The cost increased by 0.526 cm/s and the primer plot is shown in Figure 4.20, there is still a very small peak in primer magnitude in Segment 3. Therefore other times of MCM were investigated.

4.3.4.5   Adding MCM at Time of Maximum Primer Magnitude in Segment 3 for $\tau = 200°$ Case

Adding the MCM at the location of the maximum primer magnitude resulted in a cost savings, however, the duration of Segment 3 is just 0.477 days and therefore violates the half day
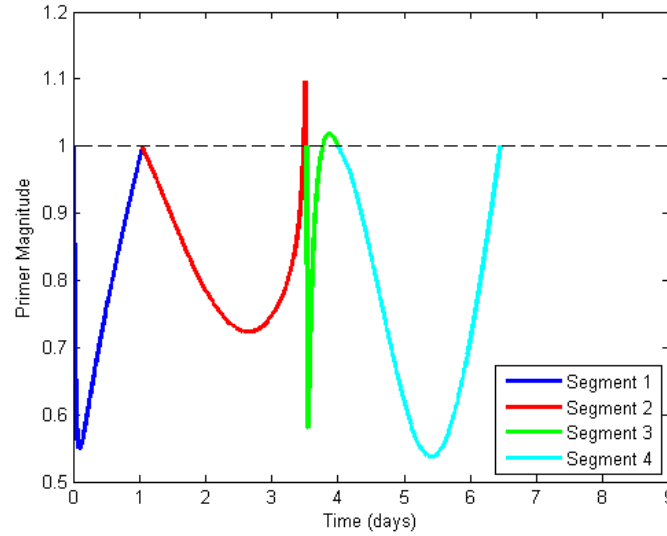
Figure 4.20: Primer Plot of MCM Added at Primer Vector Theory Calculated Location in Segment 3 for $\tau = 200°$

constraint. The details of this trajectory are in Table 4.26.

Table 4.26: MCM Added at Maximum Primer Magnitude Time in Segment 3 Details for $\tau = 200°$

ΔV Type and Segment Duration	Value
Cost Savings (m/s)	0.7086
MCM ΔV (m/s)	5.587
Segment 3 Duration (days)	0.477

4.3.4.6   Optimizer Calculate Location of MCM in Segment 3

Since the duration of Segment 3 is not long enough to satisfy the half day between burns constraint, the optimizer was used to calculate a different duration. The duration of 0.477 days was used as an initial condition with the half day between burns constraint in place. The result has a cost savings of 86.316 cm/s as seen in Table 4.27. The primer plot is shown in Figure 4.21.

Next the duration of Segment 3 was set to 1 day and allowed to vary. The final duration was 0.934 days and the cost savings found was 1.364 m/s as seen in Table 4.28. The primer plot shows that there are no more peaks in the primer magnitude. Therefore, this is a good trajectory

Table 4.27: Optimizer Calculates Time of MCM in Segment 3 for $\tau = 200°$

ΔV Type and Segment Duration	Value
Cost Savings (m/s)	0.8632
MCM ΔV (m/s)	6.326
Segment 3 Duration (days)	0.54
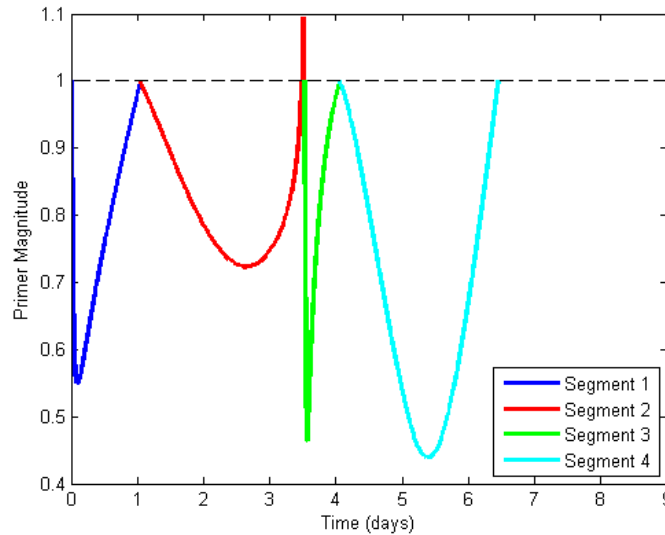
Figure 4.21: Primer Plot of Optimizer Calculates Time of MCM in Segment 3 for $\tau = 200°$

between the Moon and halo orbit, as seen in Figure 4.22.

Table 4.28: Optimizer Calculates Time of MCM, Segment 3 Duration Initialized to 1 Day for $\tau = 200°$

ΔV Type and Segment Duration	Value
Cost Savings (m/s)	1.364
MCM ΔV (m/s)	8.912
Segment 3 Duration (days)	0.93

Table 4.29: Final Cost Savings for $\tau = 200°$

Final Cost Savings and ΔV	Value
Final Cost Savings in Segment 1 and 2 (m/s)	0.00189
Final MCM ΔV in Segment 1 (m/s)	4.28e-6
Final Cost Savings in Segment 3 and 4 (m/s)	1.364
Final MCM ΔV in Segment 3 (m/s)	8.912
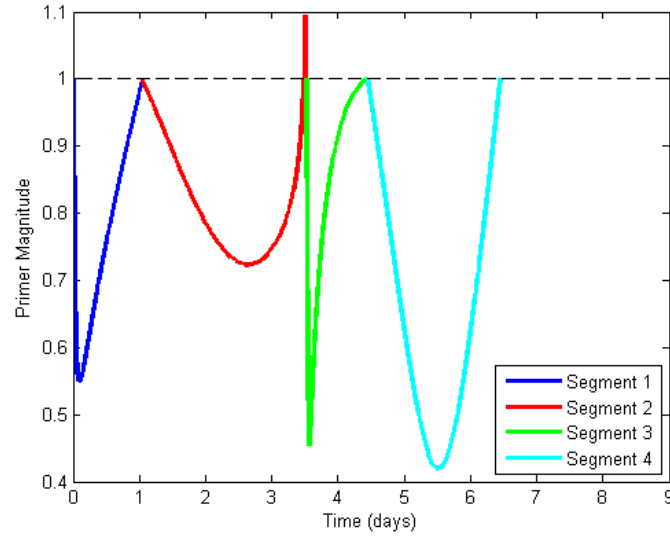
Figure 4.22: Primer Plot of Optimizer Calculated Time of MCM, Segment 3 Duration Initialized to 1 Day for $\tau = 200°$

4.3.5 Total Cost Savings from All Cases

The cost savings for each case was summed and is listed in Table 4.30. The $\tau = 60°$ case had the most cost savings, followed by the $200°$ case and then the $0°$ case.

Table 4.30: Total Cost Savings for 3 τ Angle Cases

Case	Cost Savings
$\tau=60°$ (m/s)	18.85
$\tau=0°$ (m/s)	0.164
$\tau=200°$ (m/s)	1.366

4.4 All τ Angle Trajectories

Primer plots of all of the trajectories that were built were generated to see if there are trends based on τ angle. These primer plots are in Appendix A, and the results of these plots are discussed here. First, whether a peak occurred in certain segments is examined. Figure 4.23 shows a value of 1 if the primer magnitude peaks above 1.1 within the segment listed. If there is no peak then a value of 0 is displayed. Whether a peak in primer magnitude occurs in Segment 3 and 4 is shown

in Figure 4.23(b) and if a peak occurs in Segment 6 or 7 is shown in Figure 4.23(c). Since the ΔV used to create the primer plot for Segments 8 and 9 at the Earth is not a true change in velocity, the peaks that occurred in those segments were not included.

The trajectories that entered the halo orbit at a τ angle of 320 and 340 degrees do not have any primer magnitude peaks, therefore illustrating that a mid-course maneuver is not always necessary in these trajectories. The most common peak is in Segment 2 or 3, followed by Segment 1 or 2 and then Segment 6 or 7. The total ΔV for these trajectories as well as each individual ΔV is shown in Figure 4.24.

The outbound flyby ΔV follows the trend of total ΔV the closest, and the inbound flyby also follows the general trend. The halo orbit exit burn is the most expensive for all trajectories except for $\tau = 20°$. The lowest ΔV is usually the halo orbit insertion burn or one of the flybys.

The radius of perilune of both flybys are plotted in Figure 4.25(a) and the associated ΔV for the powered lunar flyby is plotted in Figure 4.25(b). The radius of perilune of the first flyby was generally lower than the second radius of perilune, or the flyby radii were the same. While the flyby is closer on the first powered lunar flyby there is generally a higher burn than the second flyby.
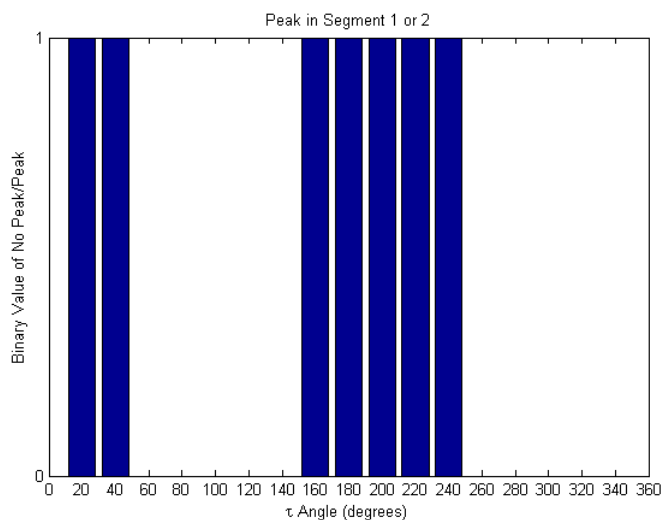
(a) τ Angle versus Segment 1 or 2 Primer Peaks
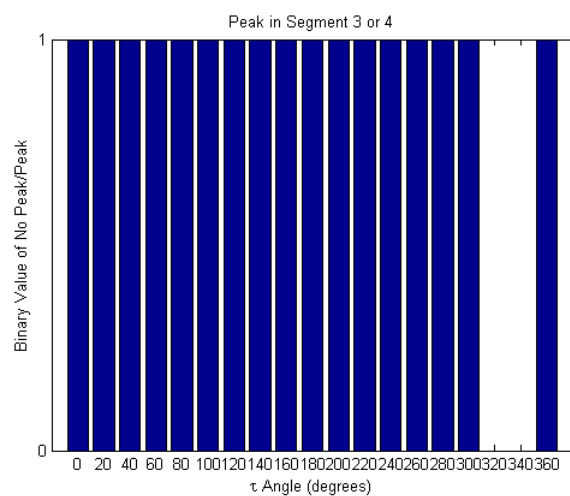
(b) τ Angle versus Segment 3 or 4 Primer Peaks
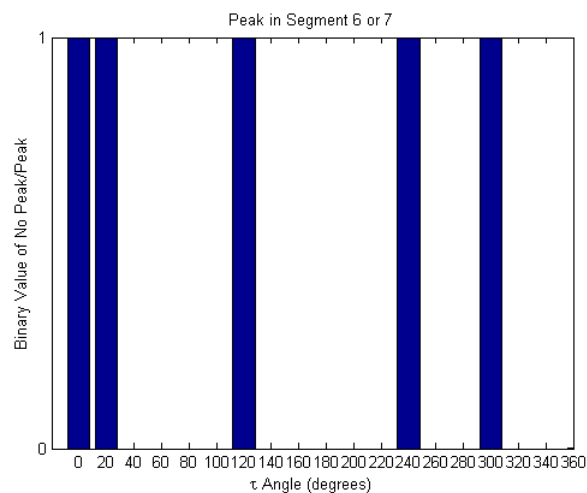
(c) τ Angle versus Segment 6 or 7 Primer Peaks

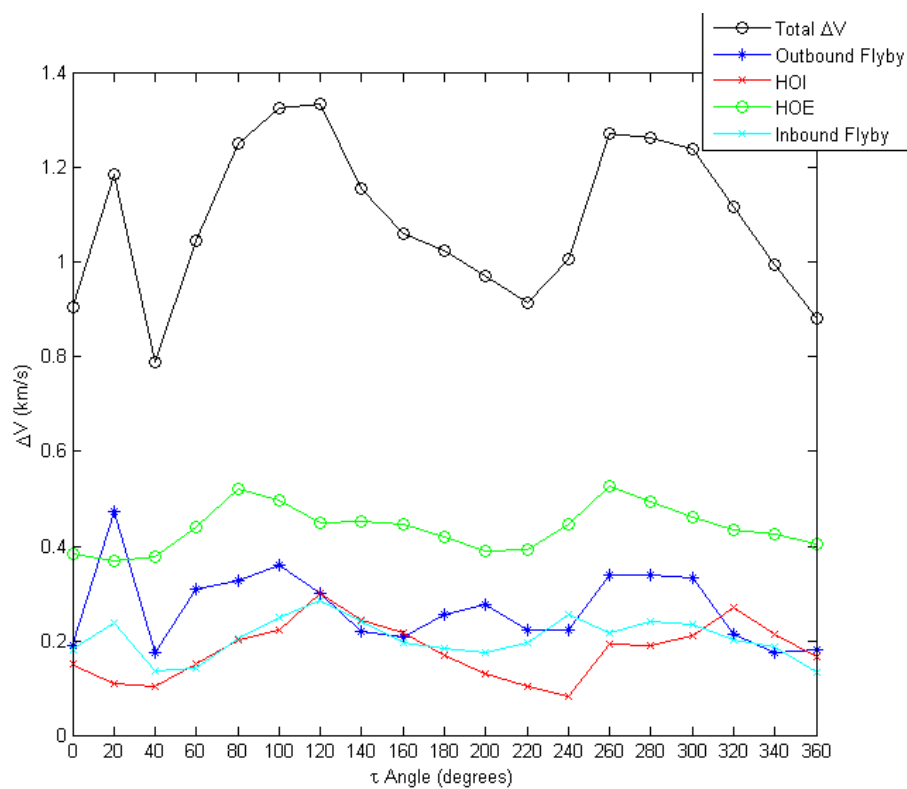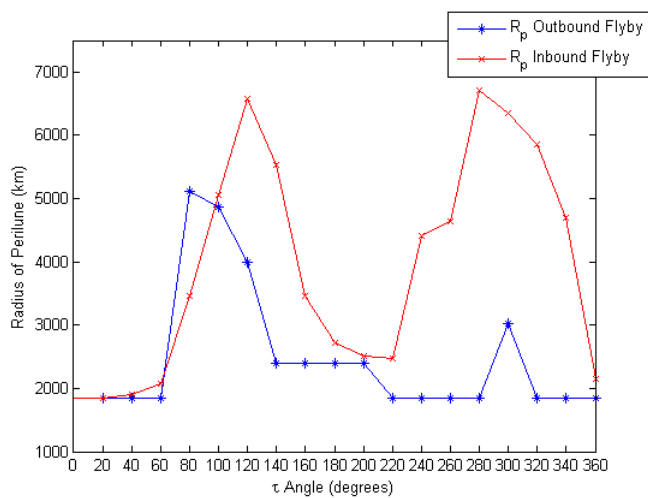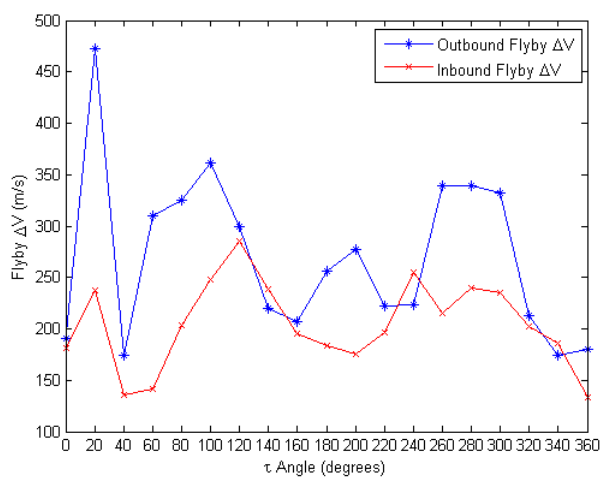Figure 4.23: τ Angle versus Segment Primer Peaks

Figure 4.24: ΔV Values for each Round Trip Trajectory that Enters Halo Orbit at Different τ Values

(a) Radius of Perilune for both Flybys

(b) Flyby ΔV's

Figure 4.25: Radius of Perilune and ΔV Values for Flybys

Chapter 5

Summary and Conclusion

5.1   Summary

Primer vector theory was applied to two different types of trajectories, Earth to halo orbit trajectories and round trip trajectories. For the Earth to halo orbit trajectories, the focus was on using the condition for optimality that states that the primer vector magnitude must not exceed unity.[11] Mid-course maneuvers were added to different trajectories to see if it resulted in cost savings; the maximum cost savings found was 8.973 m/s. Adding a mid-course maneuver where the primer plot did not indicate one was necessary was investigated by adding a MCM before the powered lunar flyby. Adding this MCM increased the total ΔV, and when the constraint on magnitude of MCM was removed, the MCM magnitude was set to zero. The primer plot still indicated that a MCM after the flyby would be beneficial even with a MCM already included. Removing the burn during the lunar flyby was also investigated. The primer plot of the resulting trajectory had a large spike in primer magnitude at the location of the lunar flyby, which indicates that the maneuver is needed. Also, the total ΔV increased drastically. Therefore, the burn at the lunar flyby is very important and should be included in these trajectories.

The round trip trajectories were built to insert into the halo orbit at certain τ values. Three cases were selected for investigation into whether mid-course maneuvers were beneficial to the trajectory. The mid-course maneuver was added in a couple of different ways. First, primer vector theory was used to calculate the location of the MCM and its magnitude. The mid-course maneuver was added at that location and the segments that it was in had to meet up at that point. If the

change in location was too great, than a continuous trajectory could not be found going to that location. If a continuous trajectory could be found, there were no cost savings. Therefore, this method of adding the MCM at the calculated location was not successful because it did not generate cost savings. Adding the mid-course maneuver at the time that the maximum primer magnitude occurred at times generated cost savings. The best method of adding the MCM was using the optimizer to select the best time for the MCM. Giving the optimizer different initial conditions of the time that the MCM occurs allowed for different solutions to be found, and then the primer plot could be examined to see if there was a better location for the MCM. At times the primer plot indicated a MCM should be added at a time that violated the half day between burn rule. The total cost savings for all of the trajectories are shown in Table 5.1.

The primer plots of all of the round trip trajectories were examined and the most common peak in primer magnitude occurred in Segment 3 and 4. A peak in Segment 1 or 2 was the second most common followed by a peak in Segment 6 or 7. Therefore, an additional impulse is needed most between the Moon and halo orbit on the outbound part of the trajectory more than an impulse between halo orbit and Moon or the return part of the trajectory.

Table 5.1: Final Cost Saving for All Trajectories

Trajectory 4	8.973 m/s
Trajectory 8	1.54 m/s
Trajectory 9	1.334 m/s
$\tau = 60°$	18.85 m/s
$\tau = 0°$	0.164 m/s
$\tau = 200°$	1.366 m/s

5.2 Future Work

This thesis illustrates how primer vector theory can be used to indicate when an additional impulse is beneficial to a trajectory. Further work can be done to investigate the trajectories that were built here and/or explore new trajectories. The round trip trajectories did not have a minimum MCM magnitude requirement. A minimum magnitude requirement could be added to see if this

alters the cost savings of the trajectories. Only three cases were selected from the 19 round trip trajectories to have mid-course maneuvers added into the trajectory. The other trajectories could be used to investigate adding mid-course maneuvers. The method of using primer vector theory to show when additional impulses are needed can be applied to different types of trajectories, either to other orbits at L_2 or to different destinations.

5.3   Conclusion

Primer vector theory is a useful tool in determining if an additional impulse could be beneficial to a trajectory. It was used on two different types of trajectories, Earth to halo orbit, and round trip trajectories. The guideline that if the primer magnitude exceeds one during the trajectory, adding an additional impulse would decrease the total cost of the trajectory, was used.[15] Primer plots indicated that for two round trip trajectories, $\tau = 320°$ and $340°$, a mid-course maneuver was not required, as well as the Earth to halo orbit trajectory, Trajectory 7. Overall, cost savings were found in the trajectories that an MCM was added to. While the cost savings were not always significant, for the $\tau = 0°$ case it was only 16 cm/s, there was still a change in the overall cost of the trajectory. For the cases where the cost savings weren't significant, this burn could be used to correct the errors of previous burns. Different methods of how to use primer vector theory were examined in the round trip trajectories. Overall, the most cost savings were found using an optimizer to calculate the time of the MCM. The primer plot of the trajectory was used to get an initial estimate of the time of the MCM but the optimizer was allowed to vary the time, and the primer plot was re-examined after the MCM was added. This was done to see if there was still a peak of primer magnitude above one and to get a new estimate of the time of the MCM. Overall, primer vector theory is a useful tool to determine when an additional impulse is needed, but an optimizer is still needed to find the best location of the MCM.

This method of using primer vector theory to find when additional maneuvers are needed could easily be applied to other types of trajectories in which mission designers are investigating whether to add additional maneuvers. Only the state transition matrix and the velocities at the

beginning and end of a trajectory are needed to generate the primer plots. From there a visual inspection and interpretation would help to understand how to make changes to make the trajectory more optimal, if necessary.

Bibliography

[1] Kring D.A. Hopkins J.B. Norris S. Joseph T. Lazio W. Kasper J. Burns, J.O. A lunar l2 farside exploration and science mission concept with the orion multi-purpose crew vehicle and a teleoperated lander \rover. Advances in Space Research, 52(2):306–320, July 2013.

[2] G. Colasurdo and D. Pastrone. Indirect optimization method for impulsvie transfers. Number 1994-3762. AIAA Astrodynamics Conference, August 1–3 1994.

[3] K. Davis. Locally Optimal Transfer Trajectories Between Libration Point Orbits Using Invariant Manifolds. PhD thesis, Department of Aerospace Engineering Sciences, University of Colorado Boulder, 2009.

[4] Farquhar R. Eismont N. Chumacenko E. Aksenov S. Fedorenko Y. Nikolaeva Y. Efremova E. Krasnopolski P. Furfaro R. Kidd J. Jr. Dunham, D.W. Some options for lunar exploration utilizing the earth moon l2 libration point.

[5] P. E. Gill, W. Murray, and M. A. Saunders. SNOPT: An SQP algorithm for large-scale constrained optimization. SIAM Review, 47(1):99–131, 2005.

[6] J.J. Guzmán. Primer vector optimization: Force model considerations. Advances in Astronautical Sciences, 120(11):1331–1345, 2005.

[7] L.A. Hiday. Optimal Transfers between Libration-Point Orbits in the Elliptic Restricted Three-Body Problem. PhD thesis, Purdue University, Purdue University, 1992.

[8] K. Hill and B.A. Jones. Turboprop version 4.0., 2009. Colorado Center for Astrodynamics Research.

[9] Jet Propulsion Laboratory, California Institute of Technology. Jpl planetary and lunar ephemerides. [http://ssd.jpl.nasa.gov/?planet_eph_export Accessed January 18, 2014], November 2011.

[10] D.J. Jezewski. Primer vector theory and applications. NASA Technical Report, NASA TR R 454, November 1975.

[11] D.J. Jezewski and H.L. Rozendaal. An efficient method for calculating optimal free-space n-impulse trajectories. AIAA Journal, 6(11):2160–2165, 1968.

[12] S.D. Hopkins J.B. Buxton C.J. Pratt W.D. Jones M.R. Kwong, J. Norris. Stepping stones: Exploring a series of increasingly challenging destinations on the way to mars. Long Beach, California, September 27-29 2011. AIAA Space Conference and Exposition.

[13] D.F. Lawden. Optimal Trajectories for Space Navigation. Butterworths and Co Publishers, London, 1963.

[14] D.F. Lawden. Rocket trajectory optimization: 1950-1963. Journal of Guidance, 14(4):705–711, 1991.

[15] P. Lion and M. Handelsman. Primer vector on fixed-time impulsive trajectories. AIAA Journal, 6(1):127–132, 1968.

[16] MathWorks. fmincon. [http://www.mathworks.com/help/optim/ug/fmincon.html Accessed April 2, 2014].

[17] C. A. Ocampo. COPERNICUS: A trajectory design and optimization system. In First International Conference on Libration Points and Libration Point Missions, Parador d'Aiguablava, Girona, Spain, 10 - 14 June 2002. Institut d'Estudis Espacials de Catalunya.

[18] A.E. Petropoulos and R.P. Russell. Low-thrust transfers using primer vector theory and a second-order penalty method. Honolulu, Hawaii, August 18–21 2008. AIAA/AAS Astrodynamics Specialist Conference and Exhibit.

[19] W. Pratt, C. Buxton, S. Hall, J. Hopkins, and A. Scott. Trajectory design considerations for human missions to explore the lunar farside from the earth-moon lagrange point em-l2. Number 2013-5478, San Diego, CA, September 10 –12 2013. AIAA SPACE 2013.

[20] J.E. Prussing. Illustration of the primer vector in time-fixed orbit transfer. AIAA Journal, 7(6):1167–1168, 1969.

[21] J.E. Prussing and J.-H. Chiu. Optimal multiple-impulse time-fixed rendezvous between circular orbits. Journal of Guidance, 9(1):17–22, January - February 1986.

[22] R.P. Russell. Primer vector theory applied to global low-thrust trade studies. Journal of Guidance, Control and Dynamics, 30(2), March-April 2007.

Appendix A

τ Angle Trajectories Primer Plots

The primer plots of all of the round trip trajectories that were created and discussed in Chapter 4.
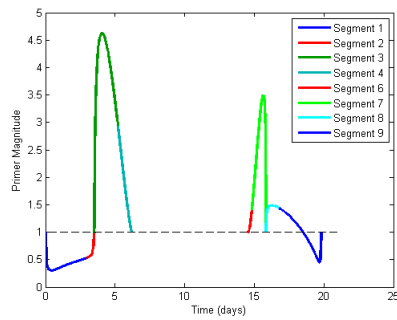
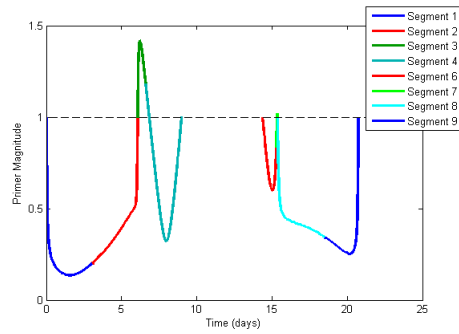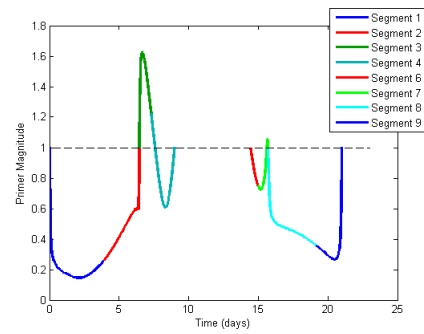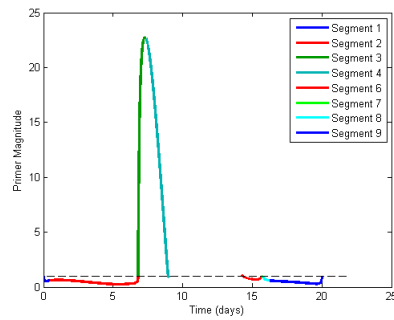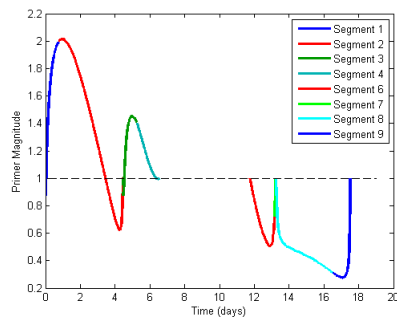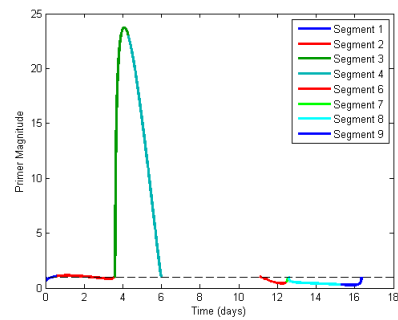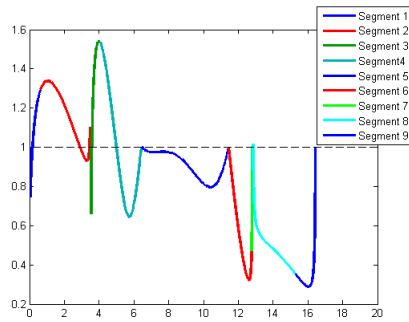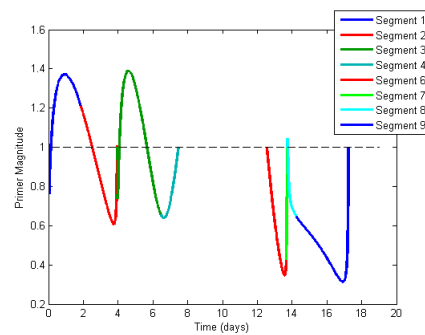(a) Primer Plot of $\tau = 0$ °
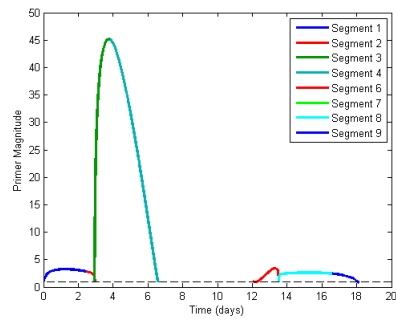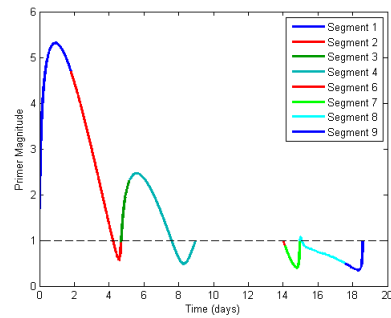
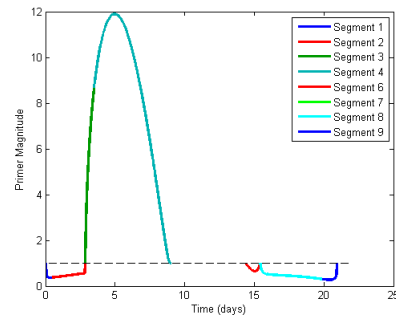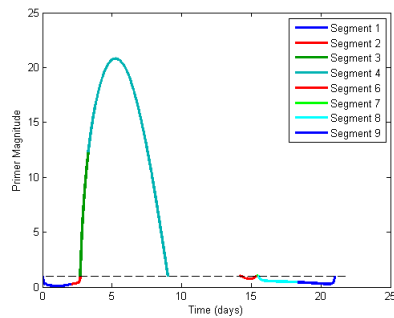(b) Primer Plot of $\tau = 20°$
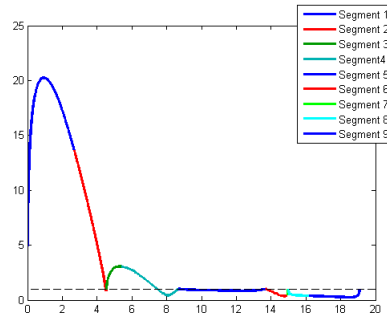
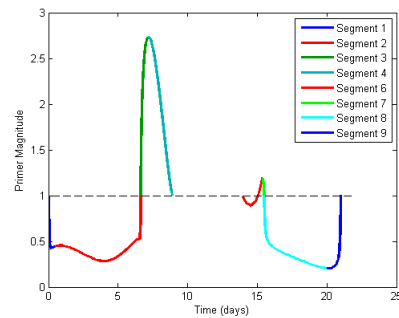(c) Primer Plot of $\tau = 40°$
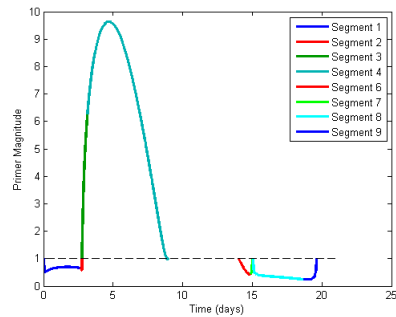
(d) Primer Plot of $\tau = 60°$

Figure A.1: Primer Plots of τ angles from $0°$ - $60°$

(a) Primer Plot of $\tau = 80$ °

(b) Primer Plot of $\tau = 100°$
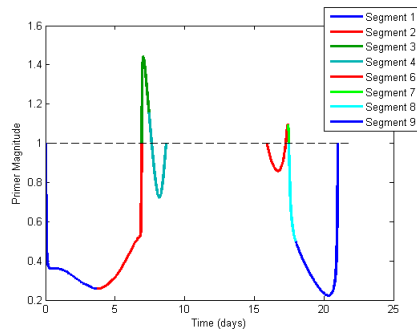
(c) Primer Plot of $\tau = 120°$

(d) Primer Plot of $\tau = 140°$

Figure A.2: Primer Plots of τ angles from $80°$ - $140°$

(a) Primer Plot of $\tau = 160$ °

(b) Primer Plot of $\tau = 180°$

(c) Primer Plot of $\tau = 200°$

(d) Primer Plot of $\tau = 220°$

Figure A.3: Primer Plots of τ angles from $160°$ - $220°$

(a) Primer Plot of $\tau = 240$ °

(b) Primer Plot of $\tau = 260°$

(c) Primer Plot of $\tau = 280°$

(d) Primer Plot of $\tau = 300°$

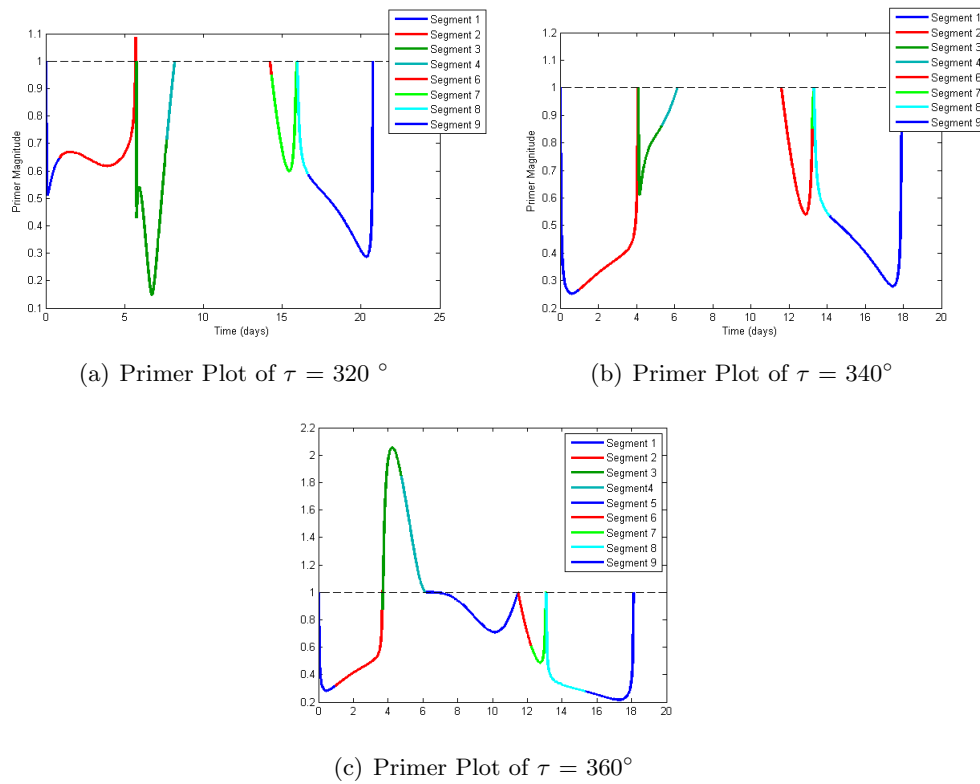Figure A.4: Primer Plots of τ angles from $240°$ - $300°$

(a) Primer Plot of $\tau = 320$ °

(b) Primer Plot of $\tau = 340°$

(c) Primer Plot of $\tau = 360°$

Figure A.5: Primer Plots of τ angles from $320°$ - $360°$